# Synthetic, Structural, Spectroscopic, and Theoretical Studies of Structural Isomers of the Cluster $Pt_3(\mu\text{-}PPh_2)_3Ph(PPh_3)_2$. A Unique Example of Core Isomerism in Phosphine Phosphido-Rich Clusters

**Robert Bender,*,† Pierre Braunstein,*,† Alain Dedieu,‡ Paul D. Ellis,§ Beth Huggins,§ Pierre D. Harvey,|| Enrico Sappa,⊥ and Antonio Tiripicchio▽**

Laboratoire de Chimie de Coordination, URA 416 CNRS, and Laboratoire de Chimie Quantique, UPR 139 CNRS, Université Louis Pasteur, 4 rue Blaise Pascal, F-67070 Strasbourg Cédex, France, Department of Chemistry, University of South Carolina, Columbia, South Carolina 29208, Faculté des Sciences, Université de Sherbrooke, Sherbrooke, Québec, Canada J1K 2R1, Dipartimento di Chimica Inorganica, Chimica Fisica e Chimica dei Materiali, Università di Torino, Via Giuria 7, I-10125 Torino, Italy, and Dipartimento di Chimica Generale ed Inorganica, Chimica Analitica, Chimica Fisica, Università di Parma, Centro di Studio per la Strutturistica Diffrattometrica del CNR, Viale delle Scienze, I-43100 Parma, Italy

*Received September 6, 1995*[⊗]

Two isomers of the phosphido-bridged platinum cluster $Pt_3(\mu\text{-}PPh_2)_3Ph(PPh_3)_2$ (**2** and **3**) have been isolated, and their structures have been solved by single-crystal X-ray diffraction. Compound **2** crystallizes in the orthorhombic space group $Cmc2_1$ with $a = 22.192(10)$ Å, $b = 17.650(9)$ Å, $c = 18.182(8)$ Å, and $Z = 4$. Compound **3** crystallizes with 2 molecules of dichloromethane in the monoclinic space group $C2/c$ with $a = 21.390(10)$ Å, $b = 18.471(9)$ Å, $c = 19.021(11)$ Å, $\beta = 105.27(5)°$, and $Z = 4$. The two isomers differ essentially in their metal−metal distances and Pt−($\mu$-$PPh_2$)−Pt angles. Thus **2**, having an imposed $C_s$ symmetry, contains a bent chain of metal atoms with two short Pt−Pt distances of 2.758(3) Å and a long separation of 3.586(2) Å. In **3**, which has an imposed $C_2$ symmetry, the metal atoms form an isosceles triangle with two Pt−Pt distances of 2.956(3) Å and one of 3.074(4) Å. These isomers can be smoothly interconverted by changing the crystallization solvents. Solution and solid-state $^{31}P$ NMR studies have been performed in order to assign the resonances of the different P nuclei and relate their chemical shifts with their structural environments. Raman spectroscopy was used to assign the $\nu$(Pt−Pt) modes of the two structural isomers. Theoretical studies based on extended Hückel calculations and using the fragment molecular orbital approach show that the isomer with the three medium Pt−Pt distances is slightly more stable, in agreement with earlier theoretical predictions. Cluster core isomerism remains a rare phenomenon, and the present example emphasizes the role and the importance of flexible phosphido bridges in stabilizing clusters as well as the unprecedented features which can be observed in phosphine phosphido-rich metal clusters.

## Introduction

The interest in the chemistry of metal clusters with bridging $\mu$-$PR_2$ groups arises in part from the electronic properties of these three-electron-donor ligands and from their unique geometrical flexibility.[1,2] The latter is evidenced by the existence of a wide range of M−($\mu$-$PR_2$)−M angles, from ca. 70 to more than 138°,[3] depending on whether metal−metal bonds are present or not. As a result of the wide variety of metals and unusual bonding situations encountered, a rich homo- and heterometallic chemistry is being developed using this and related ligands.[4] It is furthermore predictable that the phosphine phosphido-rich clusters, as yet little studied, will display new features and properties not necessarily encountered in their analogues containing better $\pi$-acceptor ligands such as carbon monoxide.

Until now, the better known and studied phosphido-bridged clusters are the trinuclear ones, which constitute, with more than a hundred examples, the largest fraction of those known. In general, triangular clusters are the smallest clusters which can be considered as models (although highly simplistic) for a metal surface, as well as the basic units for the construction of polyhedral, raftlike or stacked clusters. The platinum clusters represent a particularly fascinating class in cluster chemistry, and articles recently appeared which discuss their bonding, structures, and reactivity.[5−8] Particularly germane to the present study are the following: (i) platinum shows a remarkable tendency to form neutral or anionic clusters based on $Pt_3$ triangular arrays (e.g., the $[Pt_3(CO)_6]^{2-}$ unit has been found to be a building block for high-nuclearity stacked clusters);[9] (ii) clusters of the type $Pt_3L_{6\text{ or }7}$, which can have 42 or 44 electrons owing to the presence of low-lying orbitals of $a'_2$ and $a''_2$ symmetries (see below), are generally equilateral triangles and are stabilized when three of the ligands act as bridges between

† Laboratoire de Chimie de Coordination, Université Louis Pasteur.
‡ Laboratoire de Chimie Quantique, Université Louis Pasteur.
§ University of South Carolina.
|| Université de Sherbrooke.
⊥ Università di Torino.
▽ Università di Parma.
⊗ Abstract published in *Advance ACS Abstracts,* January 1, 1996.

(1) For review articles, see, e.g.: (a) Carty, A. J. *Adv. Chem. Ser.* **1982**, *196*, 163. (b) Garrou, P. E. *Chem. Rev.* **1981**, *81*, 229. (c) Garrou, P. E. *Ibid.* **1985**, *85*, 171. (d) Sappa, E.; Tiripicchio, A.; Braunstein, P. *Coord. Chem. Rev.* **1985**, *65*, 219. (e) Braunstein, P. *Nouv. J. Chim.* **1986**, *10*, 365. (f) Sappa, E.; Tiripicchio, A.; Carty, A. J.; Toogood, G. E. *Prog. Inorg. Chem.* **1987**, *35*, 437.
(2) Ginsburg, R. E.; Rothrock, R. K.; Finke, R. G.; Collman, J. P.; Dahl, L. F. *J. Am. Chem. Soc.* **1979**, *101*, 6550.
(3) (a) Rosenberg, S.; Geoffroy, G. L.; Rheingold, A. L. *Organometallics* **1985**, *4*, 1184. (b) Brauer, D. J.; Hessler, G.; Knüppel, P. C.; Stelzer, O. *Inorg. Chem.* **1990**, *29*, 2370.

0020-1669/96/1335-1223$12.00/0 

the metals; (iii) a large variety of ligands with different donor−acceptor abilities can be found coordinated to platinum, and this permits a comparison of the effects of different bridging or terminal ligands on the metal core structure and on the reactivity of the cluster.

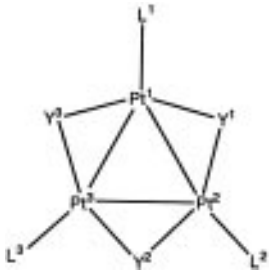

Among the elementary steps of utmost interest and of relevance to catalysis is the reversible metal−metal bond cleavage in metal dimers and clusters. This process would be expected to be favored by bridging phosphido ligands, owing to their geometrical flexibility. Reversible metal−metal bond cleavage occurring upon reversible addition of a two-electron-donor ligand has indeed been reported in several $\mu$-$PR_2$ or $\mu_3$-PR clusters.[10,11] However, one could also envisage that such a reversible process might occur in clusters exhibiting skeletal isomerism, i.e., in complexes having the same stoichiometry but different skeletal geometries in the solid state, provided these isomers are characterized by only small energy differences. Such structural isomers have been fully characterized in the cases of the butterfly and planar isomers of $[Fe_2Mo_2(\mu_3\text{-}S)_2(\eta\text{-}C_5H_5)_2(CO)_6]$[12] and of the icosahedron-derived and centered crown isomers of $[Au_9\{P(C_6H_4OMe\text{-}p)_3\}_8][NO_3]_3$.[13] However, the corresponding isomerization reactions were found to be irreversible.

**Chart 1.** Representation of the Three Isomeric Clusters $Pt_3(\mu\text{-}PPh_2)_3Ph(PPh_3)_2$ (**1**−**3**)

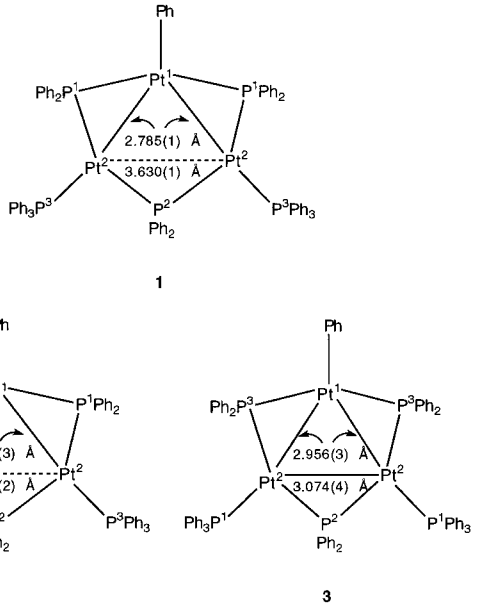


Here we report our synthetic, spectroscopic, structural, and theoretical studies on the first example of reversible skeletal isomerism in phosphido *cluster* chemistry. It involves a facile, reversible metal−metal bond cleavage in isomeric 44-electron triplatinum phosphine phosphido-rich clusters of formula $Pt_3(\mu\text{-}PPh_2)_3Ph(PPh_3)_2$, characterized by "two short and one long" (complex **2**) or by "three medium" (complex **3**) Pt−Pt distances, respectively. Yet another structural isomer of this $Pt_3$ cluster, **1**, has been reported earlier (Chart 1).[14a] More recently, a fourth isomer has been characterized as a $CH_3CN$ solvate (see Table 3).[14b] Reversible metal−metal bond cleavage has been reported for the dinuclear phosphido-bridged complex $[Rh(\mu\text{-}PBu^t_2)(CO)_2]_2$,[4h] while the bent and planar forms of $[Co(\mu\text{-}PPh_2)(CO)_3]_2$ are characterized by nonbonding Co−Co distances of 3.487(2) and 3.573(2) Å, respectively.[15] A preliminary account of the solid-state structures of **2** and **3** has appeared;[16] here we wish to discuss the structures and the electronic and spectroscopic properties of these complexes and compare their most relevant structural parameters with those of other triplatinum clusters showing closely related $Pt_3L_{6\text{ or }7}$ cores. The effects of the ligands and of their electron-donor properties are discussed on the basis of extended Hückel calculations and extend previous studies performed by Mealli[5] and Hoffmann and co-workers[6] for this type of clusters.

(4) For example: (a) Braunstein, P.; Matt, D.; Bars, O.; Loüer, M.; Grandjean, D.; Fischer, J.; Mitschler, A. *J. Organomet. Chem.* **1981**, *213*, 79. (b) Natarajan, K.; Zsolnai, L.; Huttner, G. *Ibid.* **1981**, *220*, 36. (c) Keller, E.; Vahrenkamp, H. *Chem. Ber.* **1981**, *114*, 1111. (d) Carty, A. J. *Pure Appl. Chem.* **1982**, *54*, 113. (e) Collman, J. P.; Rothrock, R. K.; Finke, R. G.; Moore, E. J.; Rose-Munch, F. *Inorg. Chem.* **1982**, *21*, 146. (f) Fultz, W. C.; Rheingold, A. L.; Kreter, P. E.; Meek, D. W. *Ibid.* **1983**, *22*, 860. (g) Haines, R. J.; Steen, N. D. C. T.; English, R. B. *J. Chem. Soc., Dalton Trans.* **1983**, 2229. (h) Jones, R. A.; Wright, T. C.; Atwood, J. L.; Hunter, W. E. *Organometallics* **1983**, *2*, 470. (i) McKennis, J. S.; Kyba, E. P. *Ibid.* **1983**, *2*, 1249. (j) Rosenberg, S.; Whittle, R. R.; Geoffroy, G. L. *J. Am. Chem. Soc.* **1984**, *106*, 5934. (k) Regragui, R.; Dixneuf, P.; Taylor, N. J.; Carty, A. J. *Organometallics* **1984**, *3*, 1020. (l) Yu, Y. F.; Gallucci, J.; Wojcicki, A. *J. Chem. Soc., Chem. Commun.* **1984**, 653. (m) Horton, A. D.; Mays, M. J.; Raithby, P. R. *Ibid.* **1985**, 247. (n) Fischer, E. O.; Filippou, A. C.; Alt, H. G.; Thewalt, U. *Angew. Chem., Int. Ed. Engl.* **1985**, *24*, 203. (o) Ritchey, J. M.; Zozulin, A. J.; Wrobleski, D. A.; Ryan, R. R.; Wasserman, H. J.; Moody, D. C.; Payne, R. T. *J. Am. Chem. Soc.* **1985**, *107*, 501. (p) Roddick, D. M.; Santarsiero, B. D.; Bercaw, J. E. *Ibid.* **1985**, *107*, 4670. (q) Gelmini, L.; Stephan, D. W. *Inorg. Chim. Acta* **1986**, *111*, L17. (r) Baker, R. T.; Tulip, T. H.; Wreford, S. S. *Inorg. Chem.* **1985**, *24*, 1379. (s) Hay, P. J.; Ryan, R. R.; Salazar, K. V.; Wrobleski, D. A.; Sattelberger, A. P. *J. Am. Chem. Soc.* **1986**, *108*, 313. (t) Targos, T. S.; Geoffroy, G. L.; Rheingold, A. L. *J. Organomet. Chem.* **1986**, *299*, 223. (u) Arif, A. M.; Jones, R. A.; Seeberger, M. H.; Whittlesey, B. R.; Wright, T. C. *Inorg. Chem.* **1986**, *25*, 3943.

(5) (a) Mealli, C. *J. Am. Chem. Soc.* **1985**, *107*, 2245. (b) For EHMO calculations on 44-electron $Pt_3$ clusters, see also: Mingos, D. M. P.; Slee, T. *J. Organomet. Chem.* **1990**, *394*, 679.

(6) Underwood, D. J.; Hoffmann, R.; Tatsumi, K.; Nakamura, A.; Yamamoto, Y. *J. Am. Chem. Soc.* **1985**, *107*, 5968.

(7) Mingos, D. M. P.; Wardle, R. W. M. *Transition Met. Chem.* **1985**, *10*, 441.

(8) Clark, H. C.; Jain, V. K. *Coord. Chem. Rev.* **1984**, *55*, 151.

(9) (a) Chatt, J.; Chini, P. *J. Chem. Soc. A* **1970**, 1538. (b) Longoni, G.; Chini, P. *J. Am. Chem. Soc.* **1976**, *98*, 7225. (c) Chini, P. *J. Organomet. Chem.* **1980**, *200*, 37.

(10) See for example: (a) Breen, M. J.; Geoffroy, G. L. *Organometallics* **1982**, *1*, 1437. (b) MacLaughlin, S. A.; Taylor, N. J.; Carty, A. J. *Ibid.* **1984**, *3*, 392. (c) Haines, R. J.; Steen, N. D. C. T.; English, R. B. *J. Chem. Soc., Dalton Trans.* **1984**, 515. (d) Jones, R. A.; Wright, T. C. *Inorg. Chem.* **1986**, *25*, 4058 and references cited therein.

(11) Huttner, G.; Schneider, J.; Müller, H.-D.; Mohr, G.; von Seyerl, J.; Wohlfarth, L. *Angew. Chem., Int. Ed. Engl.* **1979**, *18*, 76. Schneider, J.; Huttner, G. *Chem. Ber.* **1983**, *116*, 917.

(12) Braunstein, P.; Jud, J.-M.; Tiripicchio, A.; Tiripicchio Camellini, M.; Sappa, E. *Angew. Chem., Int. Ed. Engl.* **1982**, *21*, 307. Williams, P. D.; Curtis, M. D.; Duffy, D. N.; Butler, W. M. *Organometallics* **1983**, *2*, 165. Fehlner, T. P.; Housecroft, C. E.; Wade, K. *Ibid.* **1983**, *2*, 1426. Bogan, L. E., Jr.; Rauchfuss, T. B.; Rheingold, A. L. *J. Am. Chem. Soc.* **1985**, *107*, 3843.

(13) Briant, C. E.; Hall, K. P.; Mingos, D. M. P. *J. Chem. Soc., Chem. Commun.* **1984**, 290.

(14) (a) Taylor, N. J.; Chieh, P. C.; Carty, A. J. *J. Chem. Soc., Chem. Commun.* **1975**, 448. (b) Hussong, K.; Scherer, O. T. Personal communication, 1985.

(15) Harley, A. D.; Whittle, R. R.; Geoffroy, G. L. *Organometallics* **1983**, *2*, 383.

(16) Bender, R.; Braunstein, P.; Tiripicchio, A.; Tiripicchio Camellini, M. *Angew. Chem., Int. Ed. Engl.* **1985**, *24*, 861.

## Results

The transformations observed in this work are summarized in equations 1 and 2. An X-ray diffraction study was undertaken for the isomeric clusters **2** and **3**, whose results are presented

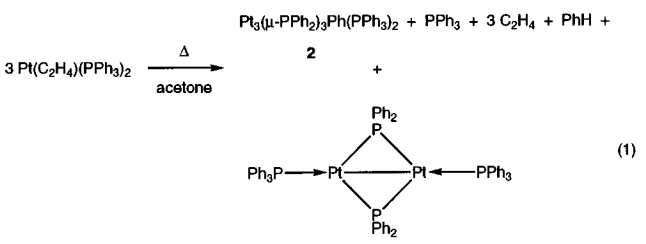


(1)

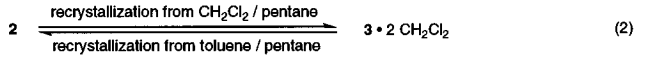


(2)

in Tables 1 and 2. Both solution and solid-state $^{31}P$ NMR studies were performed in order to relate them with the solid-state structures of these clusters. These, together with Raman studies and extended Hückel calculations, are presented in the Discussion.

## Discussion

**Synthesis and Structures of the Isomeric Clusters 2 and 3.** The nature of the ubiquitous "red platinum clusters" variously generated by pyrolysis or fragmentation of zerovalent platinum complexes such as $Pt(PPh_3)_4$ is not yet fully understood. These[14a,17−21] and related[22,23] reactions proceed by cleavage of phosphorus−carbon bonds and formation of $\mu$-$PPh_2$ and often of Pt−phenyl linkages. Such cleavage reactions induced by transition metals have received considerable attention because of their potential role in the deactivation of phosphine-containing homogeneous catalysts.[1c,24] One would anticipate that the number and the nature of the products formed will depend on the phosphine ligand, the phosphine to metal ratio, and the experimental conditions. We previously reported that refluxing an acetone solution of $Pt(C_2H_4)(PPh_3)_2$ leads to a complex mixture (eq 1) which contains *i.a.* the known[14a] diplatinum complex $Pt_2(\mu\text{-}PPh_2)_2(PPh_3)_2$, and the isomer **2** of the trinuclear cluster $Pt_3(\mu\text{-}PPh_2)_3Ph(PPh_3)_2$, which can be separated as the least soluble fraction.[16]

We have now found an easier access to **2** by refluxing a methoxyethanol solution of $Pt(C_2H_4)(PPh_3)_2$ (see Experimental Section). Cluster **2** was obtained as bright-red needles, suitable for X-ray diffraction, by recrystallization from hot acetone. Attempts to grow X-ray-quality crystals by varying the solvents led unexpectedly to the isolation of another crystalline modification: thus recrystallization from $CH_2Cl_2$/pentane at −20 °C afforded dark-red crystals of isomer **3**. Recrystallization of the latter from toluene/pentane at room temperature regenerates isomer **2**. The relationships between these isomers are shown in eq 2. The crystallization solvents are therefore of considerable importance for the isolation of a given isomer. It raises the important question of the solution structure(s) of $Pt_3(\mu\text{-}PPh_2)_3Ph(PPh_3)_2$ in various solvents (see below).

The structures of the two isomers **2** and **3** are represented in Figures 1 and 2 together with the atomic numbering systems; selected bond distances and angles are given in Tables 1 and 2. The structure of **2** has an imposed $C_s$ symmetry with the mirror plane including P(2), Pt(1), and the phenyl ring bonded to Pt(1) and shows an open triangle of Pt atoms with two short Pt(1)−Pt(2) and Pt(1)−Pt(2′) distances [2.758(3) Å] and a very long Pt(2)−Pt(2′) distance [3.586(2) Å], clearly to be considered

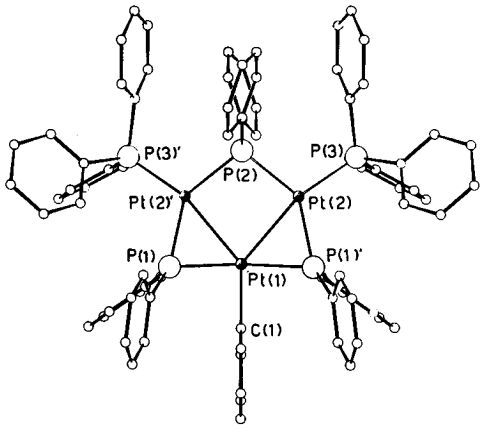


**Figure 1.** View of the molecular structure of $Pt_3(\mu\text{-}PPh_2)_3Ph(PPh_3)_2$ (**2**) with the atomic numbering scheme. The complex has an imposed $C_s$ symmetry, with the mirror plane including Pt(1), P(2), and the phenyl ring bonded to Pt(1). The phenyl groups on P(2) are disordered and distributed in two positions in such a way as to give an overall $C_s$ symmetry to the complex. Only one position of the phenyl groups is represented for clarity.

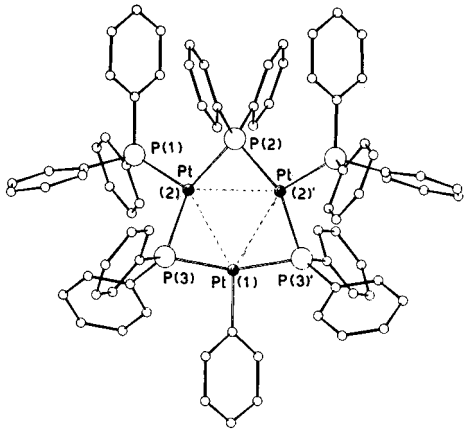


**Figure 2.** View of the molecular structure of $Pt_3(\mu\text{-}PPh_2)_3Ph(PPh_3)_2$ (**3**) with the atomic numbering scheme. The complex has an imposed $C_2$ symmetry.

**Table 1.** Selected Bond Distances (Å) and Angles (deg) in **2**[a]

| | | | |
|---|---|---|---|
| Pt(1)−Pt(2) | 2.758(3) | Pt(2)−P(2) | 2.29(1) |
| Pt(1)−P(1′) | 2.28(2) | Pt(2)−P(3) | 2.24(2) |
| | | Pt(2)−P(1′) | 2.23(2) |
| | | Pt(1)−C(1) | 1.997(4) |
| Pt(2)−Pt(1)−Pt(2′) | 81.1(1) | P(2)−Pt(2)−P(1′) | 140.2(5) |
| Pt(1)−Pt(2)−P(2) | 87.8(1) | Pt(1)−P(1)−Pt(2′) | 75.4(6) |
| P(2)−Pt(2)−P(3) | 108.2(5) | Pt(2)−P(2)−Pt(2′) | 103.1(1) |

[a] Primed atoms are related to unprimed ones by mirror symmetry (transformation: $-x, y, z$).

(17) (a) Gillard, R. D.; Ugo, R.; Cariati, F.; Cenini, S.; Bonati, F. *Chem. Commun*. **1966**, 869. (b) Ugo, R.; La Monica, G.; Cariati, F.; Cenini, S.; Conti, F. *Inorg. Chim. Acta* **1970**, *4*, 390. (c) Ugo, R.; Cenini, S.; Pilbrow, M.; Deibl, B.; Scheider, G. *Ibid*. **1976**, *18*, 113.
(18) (a) Blake, D. M.; Nyman, C. J. *J. Chem. Soc. D* **1969**, 483. (b) Blake, D. M.; Nyman, C. J. *J. Am. Chem. Soc*. **1970**, *92*, 5359.
(19) Tolman, C. A.; Seidel, W. C.; Gerlach, D. H. *J. Am. Chem. Soc*. **1972**, *94*, 2669.
(20) (a) Durkin, T. P.; Schram, E. P. *Inorg. Chem*. **1972**, *11*, 1048. (b) **1972**, *11*, 1054.
(21) Glockling, F.; McBride, T.; Pollock, R. J. I. *J. Chem. Soc., Chem. Commun*. **1973**, 650.
(22) (a) Evans, D. G.; Hughes, G. R.; Mingos, D. M. P.; Bassett, J.-M.; Welch, A. J. *J. Chem. Soc., Chem. Commun*. **1980**, 1255. (b) Jans, J.; Naegeli, R.; Venanzi, L. M.; Albinati, A. *J. Organomet. Chem*. **1983**, *247*, C37. (c) Siedle, A. R.; Newmark, R. A.; Gleason, W. B. *J. Am. Chem. Soc*. **1986**, *108*, 767.
(23) Bender, R.; Braunstein, P.; Metz, B.; Lemoine, P. *Organometallics* **1984**, *3*, 381.
(24) Dubois, R. A.; Garrou, P. E. *Organometallics* **1986**, *5*, 466. Garrou, P. E. *Chem. Rev*. **1985**, *85*, 171.

**Table 2.** Selected Bond Distances (Å) and Angles (deg) in **3**[a]

| | | | |
|---|---|---|---|
| Pt(1)−Pt(2) | 2.956(3) | Pt(2)−P(3) | 2.297(3) |
| Pt(2)−Pt(2′) | 3.074(4) | Pt(2)−P(2) | 2.252(4) |
| Pt(1)−P(3) | 2.250(4) | Pt(2)−P(1) | 2.244(4) |
| Pt(1)−C(37) | 2.01(2) | | |
| Pt(2)−Pt(1)−Pt(2′) | 62.6(1) | P(1)−Pt(2)−P(2) | 103.9(2) |
| Pt(1)−Pt(2)−Pt(2′) | 58.7(1) | P(2)−Pt(2)−P(3) | 148.5(2) |
| P(3)−Pt(1)−P(3′) | 159.8(1) | Pt(2)−P(2)−Pt(2′) | 86.1(1) |
| P(1)−Pt(2)−P(3) | 105.3(2) | Pt(1)−P(3)−Pt(2) | 81.1(1) |

[a] Primed atoms are related to unprimed ones by a 2-fold symmetry axis (transformation: $-x, y, {}^1/_2 - z$).

as a nonbonding separation. All three edges of the triangle are bridged by phosphido ligands, symmetrically for the longest one [Pt(2)−P(2) = Pt(2′)−P(2) = 2.29(1) Å, Pt(2)−P(2)−Pt(2′) = 103.1(1)°] and asymmetrically for the shortest ones [Pt(1)−P(1′) = 2.28(2) Å, Pt(2)−P(1′) = 2.23(2) Å, Pt(1)−P(1′)−Pt(2) = 75.4(6)°]. The coordination of the metal atoms is completed by two P atoms from $PPh_3$ ligands, $\sigma$-bonded to the Pt(2) and Pt(2′) atoms [Pt(2)−P(3) = Pt(2′)−P(3′) = 2.24(2) Å] and by a carbon atom of a phenyl group $\sigma$-bonded to Pt(1) [Pt(1)−C(1) = 1.997(4) Å]. The three P atoms from $PPh_2$ ligands are almost coplanar with the metals (the deviations of the P(1), P(1′), and P(2) atoms from the plane through the metals being 0.17(5), 0.17(5), and 0.08(7) Å, respectively). The structure of **2** is very similar to that of the benzene solvate $[Pt_3(\mu\text{-}PPh_2)_3Ph(PPh_3)_2]\cdot C_6H_6$ (**1**), obtained and characterized by Carty and co-workers.[14a] In the latter isomer, of imposed $C_2$ symmetry, the Pt−Pt distances are 2.785(1) and 3.630(1) Å, respectively.

The structure of **3** has a crystallographic $C_2$ symmetry with the 2-fold axis passing through the Pt(1) and P(2) atoms and shows an isosceles triangle of metal atoms with two edges of 2.956(3) and one of 3.074(4) Å. Also in this case a $PPh_2$ ligand symmetrically bridges an edge [Pt(2)−P(2) = Pt(2′)−P(2) = 2.252(4) Å, Pt(2)−P(2)−Pt(2′) = 86.1(1)°], whereas the other two asymmetrically bridge the other edges [Pt(1)−P(3) = 2.250(4), Pt(2)−P(3) = 2.297(3) Å, Pt(1)−P(3)−Pt(2) = 81.1(1)°]. The Pt(2) and Pt(2′) atoms complete their coordination through a phosphorus atom of a $PPh_3$ ligand [Pt(2)−P(1) = Pt(2′)−P(1′) = 2.244(4) Å], while Pt(1) is bonded to a carbon atom of a phenyl group [Pt(1)−C(37) = 2.01(2) Å]. The P(2) atom is in the plane of the metal atoms, whereas the P(3) and P(3′) atoms deviate from this plane by ±0.627(4) Å. The Pt−Pt distances in **3** are longer than conventional platinum−platinum bonds[25] but do not rule out the existence of metal−metal interactions.[26] Even longer $PPh_2$-bridged metal−metal distances were considered as intermediate between bonding and nonbonding in the trirhodium clusters $Rh_3(CO)_7(\mu\text{-}PPh_2)_3$ and $Rh_3(CO)_6(PPh_2H)(\mu\text{-}PPh_2)_3$, with angles at the phosphido phosphorus atom ranging from 82.9 to 89.0°.[27] Noteworthy is the different orientation of the unique phenyl group in **2** and **3**: it is orthogonal to the metal plane in the former but makes an angle of 59.2(3)° with it in the latter.

A comparison of the experimental results for the structurally characterized $Pt_3$ clusters (Table 3) leads to the following observations: (i) The 42-electron clusters are approximately equilateral, with Pt−Pt distances at the lower end of the range, unless bulky ligands are present. Thus, clusters **4**−**11** show Pt−Pt distances between 2.613 and 2.656 Å, whereas these distances range from ca. 2.660 to 2.775 Å in **18**−**20**. (ii) When $SO_2$ acts as a bridging ligand as in **16** and **17**, an increase of the Pt−Pt distances is observed: these are now between 2.695 and 2.815 Å. In cluster **14**, in particular, each Pt−Pt bond length apparently reflects the number of electrons contributed by the corresponding bridging ligand: Ph (1 $e^-$), 2.696(1) Å; $SO_2$ (2 $e^-$), 2.781(1) Å; $PPh_2$ (3 $e^-$), 2.816(1) Å. (iii) Bridging phosphido ligands increase the Pt−Pt distances, as one can see also in clusters **13** and **14** (2.75 Å). (iv) In clusters **18** and **19**, where the same bridging ligands are present, slightly longer distances are observed when the terminal ligand is a better $\pi$-acceptor. (v) A comparison between the 42-electron cluster **4** and its 44-electron counterpart **26**, which contains similar ligands, shows an increase of the Pt−Pt distances from 2.654(2) to 2.708(1) Å (average). Noting that the extra ligand in **26** is a bulky $PCy_3$, the combined electronic and steric effects only result in a relatively slight increase of the Pt−Pt distances. (vi) A comparison of the 43-electron cluster **25** with the 44-electron cluster **29**, which both have $Fe(CO)_4$ bridges, shows an increase in the Pt−Pt distances from 2.66 to 2.75 Å (average) for the isomeric mono- and dianion, respectively, suggesting an overall $Pt_3$ antibonding character for the HOMO of the latter. (vii) A comparison between the $Pt_3$ and $Pd_3$ analogues **10**/**23** and **20**/**24** indicates an average Pd−Pd bond ca. 0.02 Å longer than the Pt−Pt bond. (viii) In the phosphido-bridged complexes **31** and **32**, distances of 2.92 Å (average) are observed, suggesting that the combined effects of the increased electron count and the phosphorus bridges result in a longer metal−metal distance. (ix) Finally, the mean Pt−Pt distances for the 42-electron


(25) (a) Bender, R.; Braunstein, P.; Jud, J. M.; Dusausoy, Y. *Inorg. Chem.* **1984**, *23*, 4489. (b) Bellon, P. L.; Ceriotti, A.; Demartin, F.; Longoni, G.; Heaton, B. T. *J. Chem. Soc., Dalton Trans.* **1982**, 1671. (c) Barbier, J. P.; Bender, R.; Braunstein, P.; Fischer, J.; Ricard, L. *J. Chem. Res., Synop.* **1978**, 230; *J. Chem. Res., Miniprint* **1978**, 2913.

(26) Farrugia, L. J.; Howard, J. A. K.; Mitrprachachon, P.; Stone, F. G. A.; Woodward, P. *J. Chem. Soc., Dalton Trans.* **1981**, 1134.

(27) Haines, R. J.; Steen, N. D. C. T.; English, R. B. *J. Organomet. Chem.* **1981**, *209*, C34; **1982**, *238*, C34.

(28) Albinati, A. *Inorg. Chim. Acta* **1977**, *22*, L31.

(29) Calabrese, J. C.; Dahl, L. F.; Chini, P.; Longoni, G.; Martinengo, S. *J. Am. Chem. Soc.* **1974**, *96*, 2614.

(30) (a) Ferguson, G.; Lloyd, B. R.; Puddephatt, R. J. *Organometallics* **1986**, *5*, 344. (b) Ramachandran, R.; Yang, D.-S.; Payne, N. C.; Puddephatt, R. J. *Inorg. Chem.* **1992**, *31*, 4236. (c) See also a review article on $Pd_3$ and $Pt_3$ clusters: Puddephatt, R. J.; Manojlovic-Muir, L.; Muir, K. W. *Polyhedron* **1990**, *9*, 2767.

(31) Ferguson, G.; Lloyd, B. R.; Manojlovic-Muir, L.; Muir, K. W.; Puddephatt, R. J. *Inorg. Chem.* **1986**, *25*, 4190.

(32) Briant, C. E.; Gilmour, D. I.; Mingos, D. M. P.; Wardle, R. W. M. *J. Chem. Soc., Dalton Trans.* **1985**, 1693.

(33) Green, M.; Howard, J. A. K.; Murray, M.; Spencer, J. L.; Stone, F. G. A. *J. Chem. Soc., Dalton Trans.* **1977**, 1509.

(34) Jeffery, J. C.; Moore, I.; Murray, M.; Stone, F. G. A. *J. Chem. Soc., Dalton Trans.* **1982**, 1741.

(35) Frost, P. W.; Howard, J. A. K.; Spencer, J. L.; Turner, D. G.; Gregson, D. *J. Chem. Soc., Chem. Commun.* **1981**, 1104.

(36) Bender, R.; Braunstein, P.; Dusausoy, Y. To be published.

(37) Moody, D. C.; Ryan, R. R. *Inorg. Chem.* **1977**, *16*, 1052.

(38) Bott, S. G.; Hallam, M. F.; Ezomo, O. J.; Mingos, D. M. P.; Williams, I. D. *J. Chem. Soc., Dalton Trans.* **1988**, 1461.

(39) Scherer, O. J.; Konrad, R.; Guggolz, E.; Ziegler, M. L. *Chem. Ber.* **1985**, *118*, 1.

(40) Campbell, G. K.; Hitchcock, P. B.; Lappert, M. F.; Misra, M. C. *J. Organomet. Chem.* **1985**, *289*, C1.

(41) Freeman, M. J.; Miles, A. D.; Murray, M.; Orpen, A. G.; Stone, F. G. A. *Polyhedron* **1984**, *3*, 1093.

(42) Manojlovic-Muir, L.; Muir, K. W.; Lloyd, B. R.; Puddephatt, R. J. *J. Chem. Soc., Chem. Commun.* **1985**, 536.

(43) Francis, C. G.; Khan, S. I.; Morton, P. R. *Inorg. Chem.* **1984**, *23*, 3680.

(44) Longoni, G.; Manassero, M.; Sansoni, M. *J. Am. Chem. Soc.* **1980**, *102*, 7973.

(45) Albinati, A.; Carturan, G.; Musco, A. *Inorg. Chim. Acta* **1976**, *16*, L3.

(46) Hallam, M. F.; Howells, N. D.; Mingos, D. M. P.; Wardle, R. W. M. *J. Chem. Soc., Dalton Trans.* **1985**, 845.

(47) Arif, A. M.; Heaton, D. E.; Jones, R. A.; Nunn, C. M. *Inorg. Chem.* **1987**, *26*, 4228.

(48) Bushnell, G. W.; Dixon, K. R.; Moroney, P. M.; Rattray, A. D.; Wan, C. *J. Chem. Soc., Chem. Commun.* **1977**, 709.

(49) Berry, D. E.; Bushnell, G. W.; Dixon, K. R.; Moroney, P. M.; Wan, C. *Inorg. Chem.* **1985**, *24*, 2625.

(50) Otsuka, S.; Tatsumo, Y.; Niki, M.; Aoki, T.; Matsumoto, M.; Yoshioka, H.; Nakatsu, K. *J. Chem. Soc., Chem. Commun.* **1973**, 445.

complexes (in the range 2.62−2.74 Å, with one remarkable exception of 2.82 Å for the hydrido-rich cluster **12**) are generally lower than those for the 44-electron clusters (average 2.708−3.066 Å). In this general picture, the $PPh_2$-bridged, 44-electron clusters **1**−**3** all show Pt−Pt bonding contacts at the upper end of the range.

Clusters **2** and **3** are unique in that they display the above-mentioned reversible core isomerism. They also constitute the first example of cluster core isomerism resulting from the presence or absence of a Pt−Pt bond. Metal−metal bonded platinum dimers with a $\mu$-$PPh_2$ bridge and a terminal $C_6H_5$ ligand originating from a $PPh_3$ ligand have been reported,[22b,c] as well as other phosphido-bridged platinum dimers with Pt−Pt separations of 3.585(1) and 3.699(1) Å (and angles at $\mu$-P of 102.8(1) and 103.9(1)°, respectively).[51]

A metal−metal bonding/nonbonding isomerism has been reported for the dirhodium complex $Rh_2(CO)_4(\mu\text{-}PBu^t_2)_2$. It is accompanied yet by geometrical isomerism at the metals, giving rise to bonded tetrahedral−planar (TP) and nonbonded planar−planar (PP) forms.[4h] Interestingly, the electrochemical reduction of the PP isomer gave $[NBu^n_4]_2[Rh_2(CO)_4(\mu\text{-}PBu^t_2)_2]$, which displays a Rh−Rh bonding distance.[52] Theoretical calculations performed on the TP and PP isomers as well as on a third isomer having a Rh═Rh double bond[53] have indicated that the PP nonbonded derivative is more stable with respect to the bonded TP form by 4 kcal/mol. It is also more stable than the doubly bonded form by 7 kcal/mol. These results have been ascribed to steric factors or to the approximations used in the Hückel calculations. While the isolation of these rhodium isomers depends on the crystallization temperature, that of clusters **2** and **3** is found to depend on the crystallization solvents.

**$^{31}$P NMR Spectroscopic Studies.** The observation that different solvents allow the crystallization of dramatically different isomers exemplifies the considerable consequences that small energy differences in packing forces may have at the molecular level and raises the obvious question of the structure of the molecules in solution. Do we have a different isomer in each solvent, corresponding to or not corresponding to the solid crystallized from this solvent, or a mixture of isomers, possibly interconverting but affording only one type of molecule upon crystallization?

It is known that $^{31}$P chemical shifts of phosphido ligands are sensitive to M−P−M bond angles, where M can take on a wide range of atoms. It has also been observed that when the M−M (metal−metal) interaction is decreased or removed completely, the $\mu$-bridging phosphorus nucleus experiences what is called the upfield shift phenomenon.[1a−c,54] The changes in Pt−($\mu$-P)−Pt angles between **2** and **3**, particularly notable for P(2) (going from 103.1(1) to 86.1(1)°), led us to hope that useful information could be gained by $^{31}$P NMR spectroscopy.

**Solution Studies.** We first attempted to record the $^{31}P\{^1H\}$ NMR spectrum of each isomer in the solvent used for its crystallization, i.e. **3** in $CH_2Cl_2/CD_2Cl_2$ and **2** in acetone. In the former case, two types of signals were observed. First, a singlet resonance was seen at 10.62 ppm, flanked by satellites owing to coupling with one (two doublets of doublets) and two $^{195}$Pt nuclei, typical of a P−Pt−Pt−P arrangement ($^1J$(PtP) = 4484 Hz, $^2J$(PtP) = 252 Hz, $^3J$(PP) = 110 Hz),[25a] which is assigned to the terminal phosphine ligands. The second set of signals consists of a complex multiplet centered around *ca*. 88 ppm with overlapping satellites. It shows the pattern of an $A_2B$ spin system [$P_A$ represents P(3) in isomer **2** and P(1) in isomer **3**; $P_B$ is always P(2)] consistent with three strongly coupled phosphido nuclei. The values extracted from the spectrum are $\delta$(P(2)) 85.3 ($^1J$(PtP) = 2340 Hz, $J$(PP) = 205 Hz) and $\delta(P_A)$ 89 ($J$(PP) = 205 Hz). These solution data show the similarity between the phosphido bridges and are consistent with the solid-state structure of **3**. Note that the well-resolved and narrow lines observed indicate that no dynamic behavior is occurring around room temperature. Unfortunately, the poor solubility of **2** in acetone prevented recording of its NMR spectrum.

The solvent dependence of the phosphorus chemical shifts was examined by recording the spectrum of **3** in chlorobenzene (Figure 3). The spectrum becomes pseudo first order, with a singlet at 12.3 ppm ($^1J$(PtP) = 4500 Hz, $^2J$(PtP) = 225 Hz, $^3J$(PP) = 96 Hz), assigned to the terminal phosphines, and well separated signals for the phosphido ligands at $\delta$(P(2)) 73.6 (t, $^1J$(PtP) = 2325 Hz, $^2J$(PP) = 205 Hz) and $\delta(P_A)$ 97.9 (d, $^1J$(PtP) = 2230, 2625 Hz; $J$(PP) = 205 Hz). The shielding of P(2) by 11.7 ppm and the deshielding of $P_A$ by 8.8 ppm and of only 1.7 ppm for the terminal phosphines would be consistent with an opening of the solution structure on going from $CH_2Cl_2$ to PhCl. The same spectrum was obtained for **2** in chlorobenzene (Figure 3), showing that only one species is present in this solvent, irrespective of the solid-state structure of the isomer which was dissolved.

**Solid-State Studies.** In order to correlate spectroscopic and structural data for a given isomer, we turned to solid-state NMR spectroscopy. This technique, which is increasingly used for the study of solid-state distortions,[56] should give a direct evaluation of the sensitivity of phosphorus chemical shifts of phosphido bridging ligands to changes in their structural environment. The solid-state $^{31}$P NMR spectra of the two isomers support the molecular orbital rationale in that the most significant difference between the spectra is the chemical shift assigned to P(2). High-speed magic angle spinning spectra of the two isomers are shown in Figure 4. Assignments were based upon chemical shifts and couplings of the three types of phosphorus nuclei which give rise to three resonances consisting of a central line flanked by satellites owing to one-bond coupling with $^{195}$Pt. The resolution does not allow us to distinguish between $^1J$(PtP) values involving two chemically different $^{195}$Pt nuclei. These resonances are centered for isomer **2** around $\delta$ 16.15 ($^1J$(PtP) = 4375 Hz), 59.9 ($^1J$(PtP) = 2381 Hz), and 110.7 ($^1J$(PtP) = 2373 Hz) and for isomer **3** around $\delta$ 7.40 ($^1J$(PtP) = 4546 Hz), 82.6 ($^1J$(PtP) = 2212 Hz), and 115.8 ($^1J$(PtP) = 2357 Hz). Correlated data for P−M couplings have shown the trend of shorter M−P bond distances yielding larger $^1J$(MP) values.[54] The differences between the P(3)−Pt(2) distances in **2**, or P(1)−Pt(2) distances in **3**, and the other P−Pt bond distances are small; however, the first two bond distances are, on average, slightly shorter than the other P−Pt distances. This fact, together with the values of the chemical shifts, helped in assigning the resonances at 16.15 and 7.40 ppm, which have $^1J$(PPt) values about twice as large as the other two resonances, to the terminal phosphines of isomers **2** and **3**, respectively. These values and assignments are consistent with the solution data (see above). Also, the other two phosphorus−platinum couplings are similar, indicating that they were due to the two bridging phosphorus atoms. Given the spectrum of either isomer, one would find it difficult to assign the two most deshielded peaks. But given both spectra and the structure of

(51) Carty, A. J.; Hartstock, F.; Taylor, N. J. *Inorg. Chem.* **1982**, *21*, 1349.
(52) Gaudiello, J. G.; Wright, T. C.; Jones, R. A.; Bard, A. J. *J. Am. Chem. Soc.* **1985**, *107*, 888.
(53) Kang, S. K.; Albright, T. A.; Wright, T. C.; Jones, R. A. *Organometallics* **1985**, *4*, 666.
(54) *Phosphorus-31 NMR Spectroscopy in Stereochemical Analysis*; VCH Publishers, Inc.: Weinheim, Germany, 1987; p 559.
(55) Lee, S. W.; Trogler, W. C. *Inorg. Chem.* **1990**, *29*, 1099.
(56) See for example: (a) Carty, A. J.; Fyfe, C. A.; Lettinga, M.; Johnson, S.; Randall, L. H. *Inorg. Chem.* **1989**, *28*, 4120. (b) Rahn, J. A.; Baltusis, L.; Nelson, J. H. *Ibid.* **1990**, *29*, 750.

**Table 3.** Structural Parameters for 42−44-Electron Clusters of the Type $M_3L_{6,7}$ (M = Pd, Pt) and Related Compounds[a]

| no. | complex | M−M, Å | | | mean M−M, Å | M−M−M, deg | | | ref |
|---|---|---|---|---|---|---|---|---|---|
| | | $M^1-M^2$ | $M^1-M^3$ | $M^2-M^3$ | | at $M^1$ | at $M^2$ | at $M^3$ | |
| | 42-Electron Clusters | | | | | | | | |
| | $M^1 = M^2 = M^3 = Pt$ | | | | | | | | |
| **4** | $Pt_3(\mu\text{-CO})_3(PCy_3)_3$<br>$Y^1 = Y^2 = Y^3 = CO$; $L^1 = L^2 = L^3 = PCy_3$ | 2.656(2) | 2.656(2) | 2.653(2) | 2.654(2) | 59.9(1) | | 60.0(1) | 28 |
| **5** | $Pt_3(\mu\text{-CO})_3[PPh_2(CH_2Ph)]_3$<br>$Y^1 = Y^2 = Y^3 = CO$; $L^1 = L^2 = L^3 = PPh_2CH_2Ph$ | | | | 2.65 | | | | 29 |
| **6** | $[Pt_3(\mu_3\text{-CO})(\mu\text{-dppm})_3][PF_6]_2$ | 2.638(1) | 2.650(1) | 2.613(1) | 2.634 | 59.23(1) | 60.60(1) | 60.17(1) | 30a |
| **7** | $[Pt_3(\mu_3\text{-CO})(\mu\text{-dppm})_3](SCN)(PF_6)\cdot 2Me_2CO$[b] | 2.620(1) | 2.625(1) | 2.623(1) | 2.623 | 60.0(1) | 60.1(1) | 59.9(1) | 31 |
| **8** | $Pt_3(\mu\text{-CO})(\mu\text{-}CNC_8H_9)_2(CNC_8H_9)(PCy_3)_2$<br>$Y^2 = CO$; $Y^1 = Y^3 = CNC_8H_9$; $L^1 = CNC_8H_9$; $L^2 = L^3 = PCy_3$ | 2.627(1) | 2.625(1) | 2.648(1) | 2.633(1) | 59.76(2) | 60.56(2) | 59.68(2) | 32 |
| **9** | $Pt_3(\mu\text{-}CNC_8H_9)_3(CNC_8H_9)_2(PCy_3)$<br>$Y^1 = Y^2 = Y^3 = CNC_8H_9$; $L^1 = L^2 = CNC_8H_9$; $L^3 = PCy_3$ | 2.626(1) | 2.618(1) | 2.654(1) | 2.633(1) | 59.75(2) | 60.81(2) | 59.44(2) | 32 |
| **10** | $Pt_3(\mu\text{-}CNBu^t)_3(CNBu^t)_3$<br>$Y^1 = Y^2 = Y^3 = CNBu^t$; $L^1 = L^2 = L^3 = CNBu^t$ | 2.637(2) | 2.629(2) | 2.629(2) | 2.632(2) | 59.89(4) | 59.90(4) | 60.20(4) | 33 |
| **11** | $Pt_3[\mu\text{-C(OMe)}(C_6H_4\text{-Me-4})]_3(CO)_3$<br>$Y^1 = Y^2 = Y^3 = C(OMe)(C_6H_4\text{-Me-4})$; $L^1 = L^2 = L^3 = CO$ | 2.632(1) | 2.619(1) | 2.621(1) | 2.624(1) | 59.9(1) | 59.8(1) | 60.3(1) | 34 |
| **12** | $Pt_3(\mu\text{-H})_3H_3(PBu^t_3)_3$<br>$Y^1 = Y^2 = Y^3 = H$; $L^1 = L^2 = L^3 = PBu^t_3$; $L^1 = L^2 = L^3 = H$ | | | | 2.82(3) | | | | 35 |
| **13** | $[Pt_3(\mu\text{-H})(\mu\text{-}PPh_2)_2(PPh_3)_3]BF_4\cdot 2CH_2Cl_2$<br>$Y^2 = H$; $Y^1 = Y^3 = PPh_2$; $L^1 = L^2 = L^3 = PPh_3$ | 2.795(1) | 2.796(1) | 2.638(1) | 2.743(1) | 56.3(1) | 61.9(1) | 61.8(1) | 25b |
| **14** | $Pt_3(\mu\text{-Ph})(\mu\text{-}SO_2)(\mu\text{-}PPh_2)(PPh_3)_3$<br>$Y^1 = PPh_2$; $Y^2 = SO_2$; $Y^3 = Ph$; $L^1 = L^2 = L^3 = PPh_3$ | 2.8155(10) | 2.6958(12) | 2.7810(14) | 2.7641(14) | | | | 22a |
| **16** | $Pt_3(\mu\text{-}SO_2)_3(PPh_3)_3\cdot C_7H_8\cdot SO_2$<br>$Y^1 = Y^2 = Y^3 = SO_2$; $L^1 = L^2 = L^3 = PPh_3$ | 2.712(1) | 2.695(1) | 2.695(1) | 2.701(1) | 59.79(1) | 59.79(1) | 60.41(3) | 37 |
| **17** | $Pt_3(\mu\text{-}SO_2)_3(PCy_3)_3\cdot 2C_6H_6\cdot CH_2Cl_2$<br>$Y^1 = Y^2 = Y^3 = SO_2$; $L^1 = L^2 = L^3 = PCy_3$ | 2.814(1) | 2.813(1) | 2.815(1) | 2.814(1) | 60.04(3) | 59.96(3) | 60.00(3) | 38 |
| **18** | $Pt_3[\mu\text{-P(=}NBu^t)NBu^t(SiMe_3)]_2(\mu\text{-}CNBu^t)(CNBu^t)_3$<br>$Y^1 = Y^2 = Y^3 = P(=NBu^t)NBu^t(SiMe_3)$; $L^1 = L^2 = L^3 = CNBu^t$ | 2.731(1) | 2.697(1) | 2.660(1) | 2.696(1) | 58.7(1) | 60.0(1) | 61.3(1) | 39 |
| **19** | $Pt_3[\mu\text{-P(=}NBu^t)NBu^t(SiMe_3)]_3(CO)_3$<br>$Y^1 = Y^2 = Y^3 = P(=NBu^t)NBu^t(SiMe_3)$; $L^1 = L^2 = L^3 = CO$ | 2.745(1) | 2.747(1) | 2.732(1) | 2.741(1) | 59.7(1) | 60.2(1) | 60.1(1) | 39 |
| **20** | $Pt_3[\mu\text{-}Sn\{N(SiMe_3)_2\}_2]_3(CO)_3$<br>$Y^1 = Y^2 = Y^3 = Sn(N(SiMe_3)_2\}_2$; $L^1 = L^2 = L^3 = CO$ | 2.775(1) | 2.753(1) | 2.761(1) | 2.763(9) | 60.43(1) | | | 40 |
| **21** | $Pt_3Ir_3(\mu\text{-CO})_3(CO)_3(\eta\text{-}C_5Me_5)_3$[c,d]<br>$Y^1 = Y^2 = Y^3 = (C_5Me_5)Ir(CO)$; $L^1 = L^2 = L^3 = CO$ | 2.710(3) | 2.700(3) | 2.711(3) | 2.707(3) | 60.1(1) | 59.8(1) | 60.1(1) | 41 |
| | $M^1 = M^2 = M^3 = Pd$ | | | | | | | | |
| **22** | $[Pd_3(\mu_3\text{-CO})(\mu\text{-dppm})_3](Cl)(CF_3CO_2)\cdot H_2O$[e] | 2.584(1) | 2.585(1) | 2.603(1) | 2.591 | | | | 42 |
| **23** | $Pd_3(\mu\text{-CNCy})_3(CNCy)_3$<br>$Y^1 = Y^2 = Y^3 = CNCy$; $L^1 = L^2 = L^3 = CNCy$ | | | | 2.651(2) | | 60.0(1)[f] | | 43 |
| **24a** | $Pd_3[\mu\text{-}Sn\{N(SiMe_3)_2\}_2]_3(CO)_3$<br>$Y^1 = Y^2 = Y^3 = Sn\{N(SiMe_3)_2\}_2$; $L^1 = L^2 = L^3 = CO$ | 2.834(3) | 2.795(3) | 2.812(3) | 2.814 | 60.71(1) | | | 40 |
| **24b** | $[Pd_3(\mu\text{-NPh})_2(\mu\text{-NHPh})(PEt_3)_3]Cl$<br>$Y^1 = Y^2 = NPh$; $Y^3 = NHPh$; $L^1 = L^2 = L^3 = PEt_3$ | 2.694(2) | 2.741(2) | 2.691(2) | 2.709 | 59.3(1) | 61.2(1) | 59.4(1) | 55 |
| | 43-Electron Clusters | | | | | | | | |
| | $M^1 = M^2 = M^3 = Pt$ | | | | | | | | |
| **25** | $[N(CH_3)_3CH_2Ph][Fe_3Pt_3(CO)_{15}]$[d]<br>$Y^1 = Y^2 = Y^3 = Fe(CO)_4$; $L^1 = L^2 = L^3 = CO$ | | | | 2.656(1) | | | | 44 |

44-Electron Clusters

| | | | | | | | | | |
|---|---|---|---|---|---|---|---|---|---|
| | $M^1 = M^2 = M^3 = Pt$ | | | | | | | | |
| **1** | $Pt_3(\mu\text{-}PPh_2)_3(Ph)(PPh_3)_2 \cdot C_6H_6$<br>$Y^1 = Y^2 = Y^3 = PPh_2$; $L^1 = Ph$; $L^2 = L^3 = PPh_3$ (2 Pt−Pt) | 2.785(1) | 2.785(1) | 3.630(1) | 3.066(1) | | | | 14a |
| **2** | $Pt_3(\mu\text{-}PPh_2)_3(Ph)(PPh_3)_2$<br>$Y^1 = Y^2 = Y^3 = PPh_2$; $L^1 = Ph$; $L^2 = L^3 = PPh_3$ (2 Pt−Pt) | 2.758(3) | 2.758(4) | 3.586(2) | 3.034(4) | 81.1(1) | | | this work |
| **3** | $Pt_3(\mu\text{-}PPh_2)_3(Ph)(PPh_3)_2 \cdot 2CH_2Cl_2$<br>$Y^1 = Y^2 = Y^3 = PPh_2$; $L^1 = Ph$; $L^2 = L^3 = PPh_3$ (3 Pt−Pt) | 2.956(3) | 2.956(3) | 3.074(4) | 2.995(4) | 62.6(1) | 58.7(1) | 58.7(1) | this work |
| | $Pt_3(\mu\text{-}PPh_2)_3(Ph)(PPh_3)_2 \cdot CH_3CN$ | 2.964 | 2.964 | 3.017 | 2.982 | | | | 14b |
| **15** | $[Pt_3(\mu\text{-}Cl)(\mu\text{-}PPh_2)_2(PPh_3)_3]PF_6$<br>$Y^2 = Cl$; $Y^1 = Y^3 = PPh_2$; $L^1 = L^2 = L^3 = PPh_3$ | 2.901(1) | 2.904(1) | 2.825(1) | 2.877(1) | 58.2(1) | 60.9(1) | 60.8(1) | 36 |
| **26** | $Pt_3(\mu\text{-}CO)_3(PCy_3)_4$<br>$Y^1 = Y^2 = Y^3 = CO$; $L^1 = (PCy_3)_2$; $L^2 = L^3 = PCy_3$ | 2.714(1) | 2.736(1) | 2.675(1) | 2.708(1) | 58.78(2) | 61.02(2) | 60.20(2) | 45 |
| **27a** | $Pt_3(\mu\text{-}SO_2)_3(PCy_3)_2(dppp) \cdot 2C_6H_6$<br>$Y^1 = Y^2 = Y^3 = SO_2$; $L^1 = L^2 = PCy_3$; $L^3 = dppp$ | 2.753(1) | 2.826(1) | 2.811(1) | 2.796(1) | 60.48(4) | 61.04(4) | 58.47(4) | 46 |
| **27b** | $[Pt_3(\mu_3\text{-}H)(\mu\text{-}dppm)_3\{P(OMe)_3\}]PF_6$[g] | 2.635(1) | 2.592(1) | 2.705(1) | 2.644(1) | 62.33(2) | 58.06(2) | 59.61(2) | 30b |
| **28** | $[NEt_4][Pt_3(\mu\text{-}Br)(\mu\text{-}SO_2)_2(PCy_3)_3]$<br>$Y^1 = Y^3 = SO_2$; $Y^2 = Br$; $L^1 = L^2 = L^3 = PCy_3$ | 2.887(1) | 2.887(1) | 2.882(1) | 2.885(1) | 59.90(2) | 60.05(1) | 60.05(1) | 38 |
| **29** | $[NBu_4]_2[Fe_3Pt_3(CO)_{15}]$[d]<br>$Y^1 = Y^2 = Y^3 = Fe(CO)_4$; $L^1 = L^2 = L^3 = CO$ | | | | 2.750(1) | | | | 44 |
| | $M^1 = M^2 = M^3 = Pd$ | | | | | | | | |
| **30** | $Pd_3Cl(\mu\text{-}PBu^t_2)_3(CO)_2$<br>$Y^1 = Y^2 = Y^3 = PBu^t_2$; $L^1 = Cl$; $L^2 = L^3 = CO$ | 2.949(6) | 2.949(6) | 3.000(5) | 2.966 | 61.15(4) | 59.43(4) | 59.43(4) | 47 |
| **31** | $[Pd_3(\mu\text{-}Cl)(\mu\text{-}PPh_2)_2(PEt_3)_3][BF_4]$<br>$Y^1 = Y^3 = PPh_2$, $Y^2 = Cl$; $L^1 = L^2 = L^3 = PEt_3$ | 2.93(2) | 2.93(2) | 2.89(2) | 2.92(2) | 59.1(8) | 60.5(5) | 60.3(4) | 48,49 |
| **32** | $[Pd_3(\mu\text{-}Cl)(\mu\text{-}PPh_2)_2(PPh_3)_3][BF_4]$<br>$Y^1 = Y^3 = PPh_2$, $Y^2 = Cl$; $L^1 = L^2 = L^3 = PPh_3$ | 2.933(2) | 2.936(2) | 2.906(2) | 2.925(2) | 59.3(1) | 60.4(1) | 60.3(1) | 49 |
| **33** | $Pd_3(\mu\text{-}SO_2)_2(CNBu^t)_5 \cdot 2C_6H_6$<br>$Y^1 = Y^3 = SO_2$; $L^1 = L^3 = (CNBu^t)_2$; $L^2 = CNBu^t$ | 2.734(4) | 2.734(4) | 2.760(3) | 2.743(4) | | | | 50 |
| | $M^1 = Pt$; $M^2 = M^3 = Pd$ | | | | | | | | |
| **34** | $[Pt_{0.81}Pd_{2.19}(\mu\text{-}Cl)(\mu\text{-}PPh_2)_2(PPh_3)_3][BF_4]$<br>$Y^1 = Y^3 = PPh_2$; $Y^2 = Cl$; $L^1 = L^2 = L^3 = PPh_3$ | 2.908(1)[h] | 2.886(1)[h] | 2.878(2)[i] | | 59.6(1) | 60.6(1) | 59.8(1) | 49 |

[a] Abbreviations used: dmpm, $Me_2PCH_2PMe_2$; dppm, $Ph_2PCH_2PPh_2$; dppp, $Ph_2P(CH_2)_3PPh_2$. [b] The $SCN^-$ anion interacts significantly with one Pt atom. [c] Two independent molecules. [d] The electron count for these complexes is different, owing to the presence of heterometals. [e] The chloride anion loosely caps the metal triangle. [f] Average value. [g] The phosphite ligand is bonded to Pt(2). [h] Pd−Pt distances. [i] Pd−Pd distance.

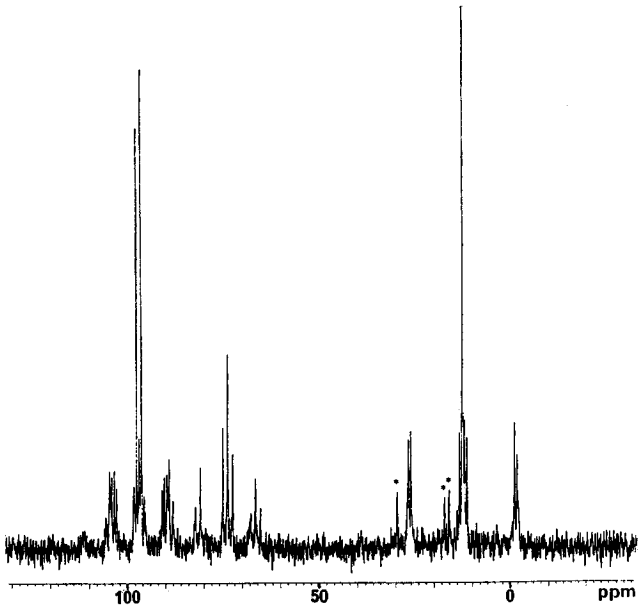


**Figure 3.** $^{31}P\{^{1}H\}$ NMR spectrum of $Pt_3(\mu\text{-}PPh_2)_3Ph(PPh_3)_2$ in chlorobenzene/$C_6D_6$. The asterisks denote impurities.

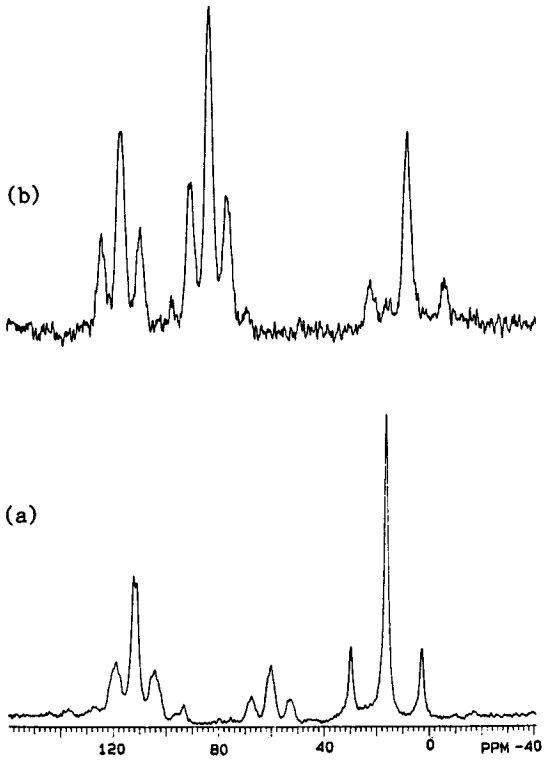


**Figure 4.** $^{31}P$ solid-state NMR spectra of (a) the 12.5 kHz MAS Bloch decay of isomer **2**, (2048 transients with no line broadening) and (b) the 12.2 kHz MAS cross-polarization of isomer **3** (8808 transients with the FID multiplied by a 50 Hz Lorentzian line broadening function). Both spectra correspond to the same spectral width.

each isomer, including bond angles, the task becomes much easier. A glance at the two spectra is enough to distinguish between the bridging phosphorus atoms. The Pt(2′)−P(2)−Pt-(2) bond angle changes by almost 3 times that of the other bridging phosphorus atom angles, while the Pt(2′)−Pt(2) bond distance increases by 0.512 Å on going from isomer **3** to **2**. It is unmistakable, then, with shifts to higher shielding of 22.7 ppm for one resonance and of 5.1 ppm for the other upon going from isomer **3** to **2**, that P(2) resonates at 59.9 ppm in isomer **2** and at 82.6 ppm in isomer **3**. This leaves the $P_A$ resonances (P(3) in isomer **2** and P(1) in isomer **3**) at 110.7 and 115.8 ppm, respectively. The final, conclusive piece of evidence lies in the relative integrals of the spectrum of **2**. This spectrum was obtained under simple Bloch decay with decoupling conditions, spinning at 12.5 kHz at the magic angle. There is relatively little overlap due to spinning sidebands, and the integrals, from deshielded to shielded, are approximately 2:1:2, for P(3):P(2):P(1). The integrals in the spectrum of isomer **3** do not reveal the same intensities because this spectrum was run under cross-polarization conditions. It was shown that the phosphorus atoms cross-polarized under different conditions and that the relative intensities of the peaks were dependent upon the contact time used for proton and phosphorus magnetization transfer. It should be noted that the chemical shift of P(2) in **2** lies outside the range usually accepted for a phosphido ligand bridging nonbonded metal atoms,[1a−c] although a $\mu$-$PPh_2$ ligand bridging Fe and Mo atoms separated by 3.891(1) Å was found to give a resonance at 92.1 ppm in solution.[4t]

Molecular orbital calculations predict, and X-ray data show, that the Pt(2)−Pt(2′) bond distance and the Pt(2)−P(2)−Pt(2′) bond angle would be the most dramatically affected in going from isomer **2** to isomer **3**. This is consistent with the change in the P(2) chemical shift being over 4 times that of the other phosphido group.

**Raman Spectroscopy: Assignment of *ν*(Pt−Pt).** The structural isomerization has also been investigated by Raman spectroscopy, particularly for the assignments of $\nu$(Pt−Pt). Firm assignments of these modes can be made via polarization[57] and resonance Raman spectroscopy[58] or via Franck−Condon analysis of the luminescence spectra.[59] Unfortunately, none of these techniques could be applied in the present case. Severe laser damage was observed for excitation wavelengths matching the strong UV−visible absorptions (e.g., 488.0 nm), and strong luminescence was observed at $\lambda_{exc} = 514.5$ nm. Furthermore, no resolution was observed in the electronic spectra. However, reasonable assignments can be made by comparing the data with literature results.

The closed structure exhibits Pt−Pt distances averaging 2.995 Å (2.956 < *r*(Pt−Pt) < 3.074 Å) and is assumed to behave as a local $D_{3h}$ $Pt_3$ local symmetry. The $Pt_3(COD)_3(\mu\text{-}SnCl_3)_2$ ($D_{3h}$) and $[Pt_3(\mu\text{-dppm})_3(CO)]^{2+}$ ($C_{3v}$) clusters exhibit $r(Pt_2)$ values of 2.58 Å[57] and 2.634 Å,[60] respectively. Their totally symmetric (mode $a_1$) and asymmetric Pt−Pt stretches (mode e) are located at 170 and 143 $cm^{-1}$ (for $Pt_3(COD)_3(\mu\text{-}SnCl_3)_2$)[57] and at 149 and 125 $cm^{-1}$ (for $[Pt_3(\mu\text{-dppm})_3(CO)]^{2+}$).[61] Because *r*(Pt−Pt) varies as $Pt_3(COD)_3(\mu\text{-}SnCl_3)_2 < [Pt_3(\mu\text{-dppm})_3(CO)]^{2+} < Pt_3(\mu\text{-}PPh_2)_3Ph(PPh_3)_2$, the $\nu$(Pt−Pt) values should vary inversely. For the closed structure (as well as the open), the $\nu$-(Pt−Pt) bands must be located below 149 $cm^{-1}$. The three candidates are 125, 112, and 96 $cm^{-1}$ (Figure 5). In order to make a choice, it is important to note that, for dimeric complexes with very similar *r*(Pt−Pt) values ($[Pt_2Cl_4(CO)_2]^{2-}$, *r*(Pt−Pt) = 2.584 Å,[62] $\nu$(Pt−Pt) = 173 $cm^{-1}$;[63] $Pt_2Cl_2(\mu\text{-dppm})_2$, *r*(Pt−Pt) = 2.699 Å,[64] $\nu$(Pt−Pt) = 150 $cm^{-1}$ [65]), the $\nu$(Pt−Pt) values

(57) See for example: Terzis, A.; Strekas, T. C.; Spiro, G. T. *Inorg. Chem.* **1971**, *10*, 2617.
(58) See for example: (a) Harvey, P. D.; Truong, K. D.; Aye, K. T.; Drouin, M.; Bandrauk, A. D. *Inorg. Chem.* **1994**, *33*, 2347. (b) Che, C. M.; Butler, L. G.; Gray, H. B.; Crooks, R. M.; Woudruff, W. H. *J. Am. Chem. Soc.* **1983**, *105*, 5492.
(59) See for example: Gray, H. B.; Rice, S. F. *J. Am. Chem. Soc.* **1983**, *105*, 4571.
(60) Ferguson, G.; Lloyd, B. R.; Puddephatt, R. J. *Organometallics* **1986**, *5*, 344.
(61) Harvey, P. D.; Hubig, S. M.; Tiegler, T. *Inorg. Chem.* **1994**, *33*, 3700.
(62) Modinos, A.; Woodward, P. *J. Chem. Soc., Dalton Trans.* **1974**, 1516.
(63) Goggin, P. L.; Goodfellow, R. J. *J. Chem. Soc., Dalton Trans.* **1973**, 2355.
(64) Brown, M. P.; Puddephatt, R. J.; Rashidi, M.; Manojlovic-Muir, L. J.; Muir, K. W.; Solomun, T.; Seddon, K. R. *Inorg. Chim. Acta* **1977**, *23*, L33.

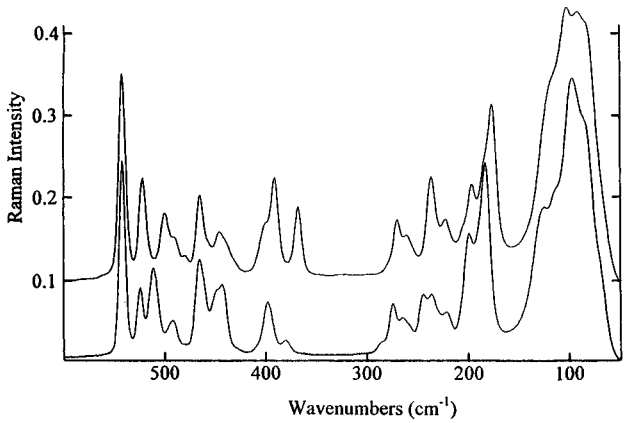


**Figure 5.** FT-Raman spectra of the solid $Pt_3(\mu\text{-}PPh_2)_3Ph(PPh_3)_2$ closed (bottom) and open structures (top). Experimental conditions: 200 scans, 4 $cm^{-1}$ resolutions. The top spectrum has been raised by 0.1 Raman unit for clarity.

are identical to $\nu(Pt-Pt)_{a1}$ in the trinuclear systems. The closest values to 2.995 Å are 2.980[66] and 3.025 Å[67] found in $[Pt_2(\mu\text{-pcp})_4]^{4-}$ (pcp = $HO(O)PCH_2P(O)OH^{2-}$) and $Pt_2(\mu\text{-dppm})_3$, respectively. In these cases, the $\nu(Pt-Pt)$ values are 113[66] and 102.5 $cm^{-1}$,[68a] respectively. The proposed assignment of $\nu(Pt-Pt)_{a1}$ for the closed structure is 112 $cm^{-1}$. This assignment would place $\nu(Pt-Pt)_e$ at 96 $cm^{-1}$. The comparison of the $\nu(a_1)/\nu(e)$ ratios for $Pt_3(COD)_3(\mu\text{-}SnCl_3)_2$, $[Pt_3(\mu\text{-dppm})_3(CO)]^{2+}$, and $Pt_3(\mu\text{-}PPh_2)_3Ph(PPh_3)_2$ (1.19, 1.19, and 1.17, respectively) is reassuring.[68b]

For the open structure, the X-ray results indicate that the cluster adopts a $C_{2v}$ geometry where the $r(Pt-Pt)$ value is 2.758 Å with a $Pt_3$ angle of 98.9°. Due to the shorter $r(Pt-Pt)$ value, the $\nu(Pt-Pt)$ data should be localized above 112 $cm^{-1}$. The only candidate is the 122 $cm^{-1}$ band which appears as an intense and broad shoulder (Figure 5). It is assumed that the 125 $cm^{-1}$ component observed in the closed structure (Figure 5) is included in the total intensity of this 122 $cm^{-1}$ feature (explaining, in part, the gain in relative intensity). The other $\nu(Pt-Pt)$ mode can be assigned to the 105 $cm^{-1}$ peak, a peak that is not present in the closed-structure spectrum (Figure 5).

Using a recently reported empirical relationship relating $r(Pt-Pt)$ (in Å) and $F(Pt-Pt)$ (in mdyn·$Å^{-1}$)[58a]

$$r(Pt-Pt) = -0.223 \ln F(Pt-Pt) + 2.86 \qquad (3)$$

the $F(Pt-Pt)$ values estimated for the closed (2.995 Å) and open (2.758 Å) structures are 0.55 and 1.58 mdyn·$Å^{-1}$, respectively. Finally, when the long Pt···Pt interactions of the open structure (3.586 Å) are considered, eq 3 predicts a value of 0.039 mdyn·$Å^{-1}$ for $F(Pt\cdots Pt)$.

**Theoretical Analysis.** Hoffmann's calculations[6] show that, in the triangular $Pt_3(\mu\text{-}Y)_3L_3$ 42-electron clusters, of $D_{3h}$ symmetry, the HOMO ($a'_1$ symmetry) is metal−metal bonding in character. The LUMO, 1−2 eV higher in energy, lying in the plane of the triangle and having $a'_2$ or $a''_2$ symmetry depending on the nature of the bridging ligands, has an important metal−bridging ligand component ($\sigma$ for $a'_2$ or $\pi$ for $a''_2$) with a smaller metal−metal antibonding character. It can be foreseen that the passage from 42 to 44 valence electrons with occupation of the latter orbital will result in a lengthening of the Pt−Pt bond distances. This is experimentally verified (see above). In the 44-electron clusters with $\pi$-donor bridging ligands (halides or phosphides), the filled frontier orbitals are of $a'_1$ (Pt−Pt bonding) and $a'_2$ (Pt−Pt antibonding in character) symmetries. Calculations show also that a closed structure of $D_{3h}$ symmetry remains the most stable. However, a deformation with the opening of one Pt−Pt bond leading to a $C_{2v}$ symmetry was found to require only little energy. Mealli comes to similar conclusions and emphasizes that occupation of the Pt−Pt antibonding $a'_2$ level weakens the metal−metal bond but does not destroy it.[5a] This weakened bond would then have a bond order of $^2/_3$. Molecular orbital calculations performed on complex **1** show that the total energy is minimized for a $D_{3h}$ symmetry, although its solid-state structure is of $C_{2v}$ symmetry, the opening of one Pt−Pt−Pt angle from 60 to 85° still requiring 25 kcal/mol.

Rather than focusing on the amount of energy needed to open or to close a Pt−Pt bond—extended Hückel calculations are probably not well suited for this task—one would like to go one step further and rationalize the existence of the two different isomers **2** and **3**. A better understanding of the factors which account for this situation would be also of interest for designing syntheses of similar systems. As the above mentioned theoretical analyses[5,6] of the orbital patterns for these 44-valence-electron clusters have provided a rationale of their stability, we shall not repeat here similar arguments but rather concentrate on the assessment of the factors which govern the relative stability of the two isomers. Our discussion will be also based on extended Hückel calculations,[69] details of which are given in the Experimental Section, using the fragment molecular orbital approach.[70] This approach was particularly useful to unravel the very intricate interactions which arise from strong mixing between orbitals of the same symmetry and of similar energies. The orbital picture that we will discuss here is therefore a simplified one, but it presents all essential features.

Before going into the discussion, let us first mention two points: (i) Steric reasons may be invoked to rationalize the distortion from $D_{3h}$ symmetry toward $C_{2v}$ symmetry. Yet that the *same* system exhibits both geometries is more difficult to reconcile with purely steric arguments. (ii) This situation seems to be peculiar to a nonsymmetric $Pt_3L_2L'$ core, L′ being a rather strong $\sigma$-donor ligand. In this case, it is the metal−metal bond opposite to the L′ ligand which can open. On the other hand, 44-valence-electron clusters of the type $Pt_3(\mu\text{-}Y)_3L_3$ having a symmetric $Pt_3L_3$ core all display a closed geometry.

Calculations carried out for the model system $Pt_3(\mu\text{-}PH_2)_3R(PH_3)_2$ where $PH_3$ and $PH_2$ stand as models for the triphenylphosphine and diphenylphosphido ligands, respectively, do indeed reflect the experimental trend, as discussed above. As shown in Table 4, the energy difference between the closed and open geometries decreases along the series R = $PH_3^+$, $CH_3$, $C_6H_5$, the closed geometry being always more stable than the open one.

We shall therefore analyze successively the $[Pt_3(\mu\text{-}PH_2)_3(PH_3)_3]^+$ and $Pt_3(\mu\text{-}PH_2)_3(CH_3)(PH_3)_2$ systems for each isomer. Their orbitals may be obtained by interacting the orbitals of the $Pt_3L_3^{4+}$ core with the orbitals of the system made of the three bridging $PH_2^-$ ligands. As stated above, we shall not

(65) Alves, O. L.; Virtorge, M.-C.; Sourisseau, C. *Nouv. J. Chim.* **1983**, *7*, 231.
(66) King, C.; Auerbach, R. A.; Fronczek, F. R.; Roundhill, D. M. *J. Am. Chem. Soc.* **1986**, *108*, 5626.
(67) (a) Manojlovic-Muir, L. J.; Muir, K. W. *J. Chem. Soc. Chem. Commun.* **1982**, 1155. (b) Manojlovic-Muir, L.; Muir, K. W.; Grossel, M. C.; Brown, M. P.; Nelson, C. D.; Yavari, A.; Kallas, E.; Moulding, R. P.; Seddon, K. R. *J. Chem. Soc., Dalton Trans.* **1985**, 1955.
(68) (a) Harvey, P. D.; Gray, H. B. *J. Am. Chem. Soc.* **1988**, *110*, 2145. (b) For comparison, $Pt_3$ vibrational frequencies for $[Pt_3(CO)_6]^{2-}$ have been estimated at 191, 161, and 112 $cm^{-1}$: Grushow, A.; Ervin, K. M. *J. Am. Chem. Soc.* **1995**, *117*, 11612.
(69) (a) Hoffmann, R. *J. Chem. Phys.* **1963**, *39*, 1397. (b) Hoffmann, R.; Lipscomb, W. N. *Ibid.* **1962**, *36*, 3179; **1962**, *37*, 2872.
(70) (a) Hoffmann, R. *Science* **1981**, *211*, 995. (b) See also: Albright, T. A.; Burdett, J. K.; Whangbo, M. H. *Orbital Interactions in Chemistry*; J. Wiley and Sons: New York, 1985.

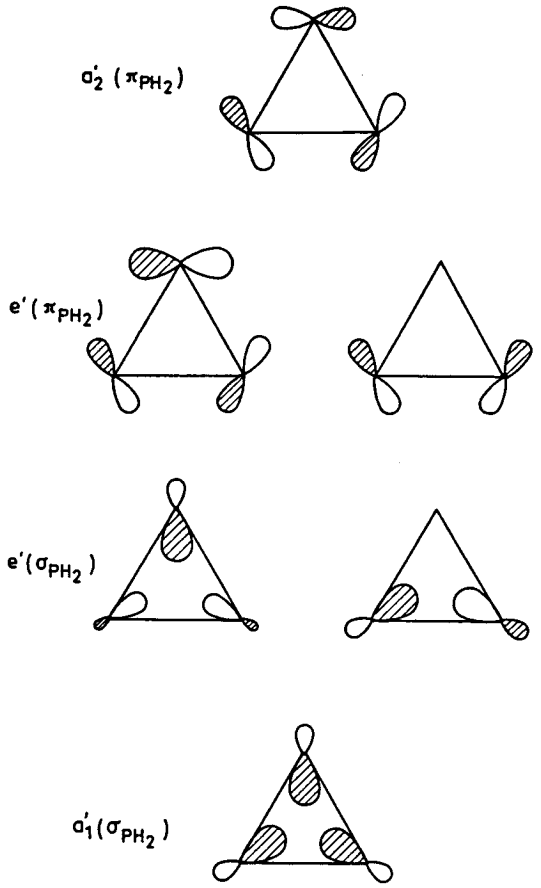


**Figure 6.** Basic orbitals of the $(PH_2)_3^{3-}$ fragments.

derive all these orbitals here, since our purpose is not to trace the interactions which account for the intrinsic stability of the clusters, but we shall rather focus on the interactions which are important for the relative stability of the two possible isomers.

Let us first recall the basic orbitals of the $(PH_2)_3^{3-}$ fragments. As seen in Figure 6, they consist of a set of symmetry-adapted in-plane combinations of the $\sigma$ orbitals ($a'_1(\sigma(PH_2))$ and $e'(\sigma(PH_2))$ and of another set of the symmetry-adapted in-plane combinations of the $\pi$ orbitals ($a'_2(\pi(PH_2))$ and $e'(\pi(PH_2))$ (we refer here to the plane of the $Pt_3$ core). Taking the phosphido bridge as a $PH_2^-$ anion results in having all these levels occupied.

The levels of the $[Pt_3(PH_3)_3]^{4+}$ core are quite similar to the levels of the $[Pt_3(CO)_3]^{4+}$ system,[5,6] with the exception of the low-lying $\pi^*_{CO}$ orbitals which are absent here. The HOMO **I**,

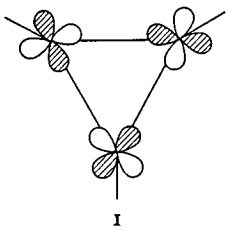


of $a'_2$ symmetry, is an antibonding combination of d$\pi$ orbitals of the three $Pt(PH_3)$ units. Somewhat above and unoccupied, one finds a set of two degenerate levels of e′ symmetry, e′ (d$\sigma$), which originate from the d$\sigma$ orbitals of the $Pt(PH_3)$ unit. These two levels are *schematically* sketched in **II** and **III**. A better and more acurate representation is given by the corresponding contour diagrams shown in Figures 7 and 8. A feature appearing in these contour diagrams which will be important in the following discussion is that the equatorial lobes of these orbitals

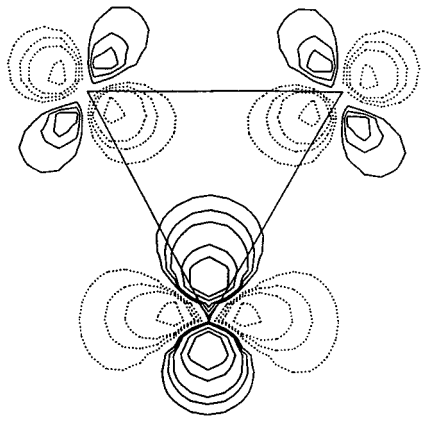

**Figure 7.** Contour diagram of the e′(d$\sigma$) orbital schematically represented in (**II**) in the text.

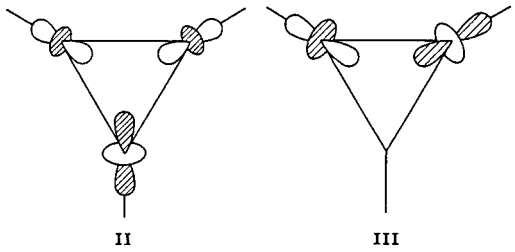


spread quite extensively out of the $Pt_3$ triangle. This is due to the strong $d_{z^2}/d_{x^2-y^2}$ mixing.

If one now puts together the two fragments $[Pt_3(PH_3)_3]^{4+}$ and $(PH_2)_3^{3-}$, the two empty levels **II** and **III** find e′($\pi$($PH_2$)) and e′($\sigma$($PH_2$)) as interacting counterparts. The corresponding interactions, shown in **IV**−**VII**, are two electron-stabilizing ones.

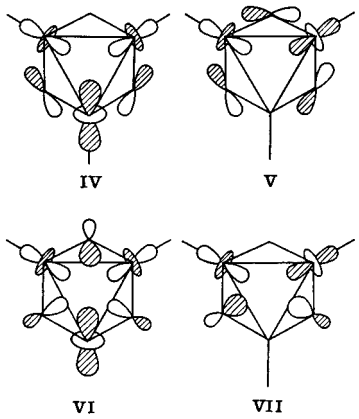


The phase relationship is determined by the interaction with the equatorial lobe of the d$\sigma$ Pt orbital since, as mentioned above, these equatorial lobes point toward the phosphido group and are quite important in size. The interactions **IV**−**VII** are quite large due to a substantial overlap ($\langle e'(d\sigma)|e'(\pi(PH_2))\rangle = 0.182$ and $\langle e'(d\sigma)|e'(\sigma(PH_2))\rangle = 0.216$). There are of course many other interactions[5,6] but **IV**−**VII** are the ones which are, as we shall now see, decisive for the relative stability of the closed and open isomers.[71]

When the Pt−Pt−Pt angle increases from 60 to 81° (the experimental value in the open form **2** of the title system), the energy levels of the $[Pt_3(\mu\text{-}PH_2)_2(PH_3)_3]^+$ system vary (some of them being, for instance, allowed to mix due to the lowering of the symmetry from $D_{3h}$ to $C_{2v}$) but the basic interaction

(71) As stated in the text, orbitals **IV**−**VII** correspond to a schematic deconvolution of strongly mixed orbitals having the same symmetry and close in energy. We cannot therefore provide useful corresponding contour diagrams.

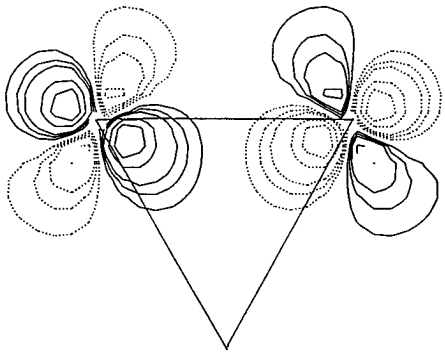

**Figure 8.** Contour diagram of the e′(d$\sigma$) orbital schematically represented in (**III**) in the text.

**Table 4.** Destabilization of the Open Form with Respect to the Closed Form as a Function of the Ligand R in $Pt_3(\mu\text{-}PH_2)_3R(PH_3)_2$

| R | $\Delta E$, kcal/mol |
|---|---|
| $PH_3^+$ | 16.9 |
| $CH_3$ | 8.2 |
| $C_6H_5$ | 4.7 |

pattern is not substantially affected. Yet the whole system is destabilized (see Table 4) by 16.9 kcal/mol: some steric factors may be at work but the stabilizing interactions mentioned above are also decreased, especially for **VI** and **VII**, where the corresponding overlaps are now respectively 0.174 and 0.171 instead of 0.216.

If one now replaces one $PH_3$ ligand in the closed isomer with a better $\sigma$ donor, e.g., $CH_3$, the degeneracy of the e′(d$\sigma$) levels is lifted. As shown below, **II** is destabilized somewhat and, more importantly, becomes localized on the Pt−$CH_3$ unit; see **VIII**.

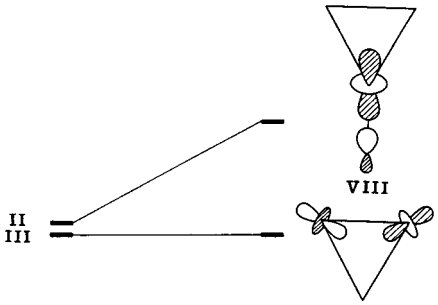


On the other hand, **III** is not affected by the replacement. The corresponding overlaps with e′($\sigma$ $PH_2$) also reflect the modification of **II**. One has an overlap of 0.228 for the interaction sketched in **IX**. If one opens the Pt−Pt−Pt angle,

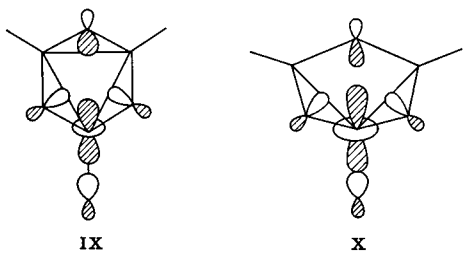


**IX** → **X**, the overlap now *increases* up to 0.240. Remember that in $Pt_3(\mu\text{-}PH_2)_3(PH_3)_3$ the overlap between e′($\sigma$ $PH_2$) and e′(d$\sigma$) was decreasing. Thus **X** is more stabilizing than **IX**, and the calculated overall destabilization of the open form with respect to the closed form is comparatively less in $Pt_3(\mu\text{-}PPh_2)_3CH_3(PPh_3)_2$ than in $[Pt_3(\mu\text{-}PPh_2)_3(PPh_3)_3]^+$ (see Table 4). The increase in the overlap is traced to the greater localization of **II** on the Pt−$PH_3$ unit opposite to the opening bond. It follows that the greater the $\sigma$ strength is, the greater the localization, the greater the increase in the overlap, and the greater the stabilizing interaction **X** (the overlap increases from 0.228 to 0.240 for $CH_3$ and from 0.216 to 0.240 for $C_6H_5$). This explains that the destabilization of the open form with respect to the closed form decreases along the series $PH_3^+$, $CH_3$, $C_6H_5$ (see Table 4).

Finally, one might wonder what would be the effect of the replacement of the three phosphine ligands by three equivalent but better $\sigma$ donor ligands.[72] Somewhat surprisingly, the energy difference betweeen the two isomers is again rather high, amounting to 19.3 kcal/mol for the $[Pt_3(\mu\text{-}PH_2)_3(CH_3)_3]^{2-}$ model system. A look at the two wave functions and at the orbital overlap of interest indicates that the $\langle e'(d\sigma)|e'(\sigma\ PH_2)\rangle$ overlap decreases again from 0.246 in the closed isomer to 0.216 in the open one, thus accounting for the decrease in the stabilization provided by the $\sigma(d_{z^2})$ levels.

It therefore appears from this analysis that the asymmetry of the $Pt_3$ core brought about by the replacement of one phosphine ligand by a better $\sigma$-donor ligand is at the origin of the existence of two different isomers in this class of compounds.

## Experimental Section

All manipulations were performed under nitrogen by using standard Schlenk techniques. The solvents used were dried and distilled prior to use by using conventional procedures.[4a] The $^{31}P\{^1H\}$ NMR spectra were measured on a FT-Bruker WP-200 SY instrument at 81.02 MHz or on a FT-Bruker AM-400 instrument at 161.98 MHz. The $^{31}P$ solid-state NMR spectra were run at 161.98 MHz on a Varian XL-400 spectrometer, at room temperature. The solid samples were spun at 12.2−12.5 kHz in a 5-mm high-speed-spinning, broad-band probe made by Doty Scientific. Chemical shifts are referenced to 85% $H_3PO_4$.

**Synthesis of $Pt_3(\mu\text{-}PPh_2)_3Ph(PPh_3)_2$.** In a typical experiment, a methoxyethanol solution (120 mL) of $Pt(C_2H_4)(PPh_3)_2$ (12.40 g, 16.6 mmol), prepared according to the literature,[73] was refluxed for 3 h. The solvent was removed under reduced pressure, and the dry residue was washed with cold acetone until the solution became colorless. The bright red, very poorly soluble solid residue of **2** was dried in vacuo (2.90 g, 30% based on Pt). This analytically pure microcrystalline powder may be recrystallized from hot acetone. Anal. Calc for $C_{78}H_{65}P_5Pt_3$ (**2**) ($M$ = 1742.5): C, 53.76; H, 3.76. Found: C, 53.78; H, 3.78.

Slow diffusion of hexane in a $CH_2Cl_2$ solution of **2** afforded dark red crystals of $Pt_3(\mu\text{-}PPh_2)_3Ph(PPh_3)_2\cdot 2CH_2Cl_2$ (**3**). Anal. Calc for $C_{80}H_{69}Cl_4P_5Pt_3$ ($M$ = 1912.4): C, 50.24; H, 3.62. Found: C, 50.28; H, 3.62.

**X-ray Crystallography.** A bright-red needle of **2** and a dark-red prismatic crystal of **3** were selected for the X-ray analysis. All crystals of **2** were small and were of poor quality (efforts to grow crystals of **2** from other solvents led to crystals of **3**). The needle of **2** selected for the X-ray analysis diffracted very weakly so that only a limited number of observed reflections (although all those with $I > \sigma(I)$ were considered observed) could be obtained, which proved to be sufficient to solve the structure unambiguously but prevented an accurate refinement to be performed.

The crystallographic data for both **2** and **3** are given in Table 5. Unit cell parameters were obtained by least-squares refinement of the $\theta$ values (in the ranges 9−13 and 10−16° for **2** and **3**, respectively) of 21 (**2**) and 30 (**3**) carefully centered reflections chosen from different regions of the reciprocal space. Data were collected at room temperature, the individual reflection profiles having been analyzed according to Lehmann and Larsen.[74] The structure amplitudes were obtained after usual Lorentz and polarization reduction.[75] A correction for absorption effects was applied only to **3** (maximum and minimum transmission

(72) This was suggested to us by R. Hoffmann.
(73) Nagel, U. *Chem. Ber.* **1982**, *115*, 1998.
(74) Lehmann, M. S.; Larsen, F. K. *Acta Crystallogr., Sect. A*: *Cryst. Phys. Diffr., Theor. Gen. Crystallogr.* **1974**, *A30*, 580−584.
(75) Sheldrick, G. M. SHELX Program for Crystal Structure Determination. University of Cambridge, England, 1976.

**Table 5.** Experimental Data for the X-ray Diffraction Study of **2** and **3**

| | **2** | **3** |
|---|---|---|
| formula | $C_{78}H_{65}P_5Pt_3$ | $C_{78}H_{65}P_5Pt_3 \cdot 2CH_2Cl_2$ |
| fw | 1742.51 | 1912.38 |
| cryst system | orthorhombic | monoclinic |
| space group | $Cmc2_1$ | $C2/c$ |
| $a$, Å | 22.192(10) | 21.390(10) |
| $b$, Å | 17.650(9) | 18.471(9) |
| $c$, Å | 18.182(8) | 19.021(11) |
| $\beta$, deg | | 105.27(5) |
| $V$, Å$^3$ | 7122(6) | 7250(7) |
| $D_c$, g cm$^{-3}$ | 1.625 | 1.752 |
| $Z$ | 4 | 4 |
| $T$, °C | 25 | 25 |
| radiation | Nb-filtered Mo Kα ($\lambda = 0.710\ 73$ Å) | |
| $\mu$, cm$^{-1}$ | 60.90 | 61.35 |
| final $R$ and $R_w$ indices[a] | 0.080, 0.098 | 0.045, 0.055 |

[a] $R = \sum(|F_o| - |F_c|/\sum|F_o|$; $R_w = [\sum w(|F_o| - |F_c|)^2/w|F_o|^2]^{1/2}$.

factors 1.2447 and 0.7927).[76] Only the observed reflections were used in the structure solution and refinement. Both structures were solved by using conventional Patterson and Fourier techniques. Of the two possible space groups $C2/c$ and $Cc$ for **3** from the systematic absences ($h0l$ with $l = 2n$), $C2/c$ was chosen and confirmed by the structure determination. From the systematic absences for **2** ($h0l$ with $l = 2n$), three space groups were possible: $Cmc2_1$, $C2cm$, and $Cmcm$. Initially, the choice of the space group presented some difficulties, as the positions of the Pt and P atoms roughly agreed with all three space groups, this atomic frame showing an approximate $C_{2v}$ symmetry. The $Cmc2_1$ space group was chosen from the structure determination because the complex as a whole displayed only a mirror plane passing through Pt(1), P(2), and the phenyl ligand at C(1). The phenyl groups of the phosphido ligand bridging the long edge of the platinum triangle in **2** were found disordered and distributed in two positions of equal occupancy in such a way as to give an overall $C_s$ symmetry to the complex. The positions of these disordered phenyl groups and those of the phenyl bonded to the Pt atom were clearly located in the Fourier maps, but their refinement did not give good results, so that they were introduced in the calculations with fixed thermal parameters but not refined. In the last cycles of the refinement (by full-matrix least-squares), the other phenyl groups were treated as rigid groups of $D_{6h}$ symmetry with C−C bonds of 1.395 Å and anisotropic thermal parameters were used for the Pt and P atoms only.

The electron density map of **3** showed additional molecules of solvation. In the last cycles of refinement, carried out by full-matrix least-squares, anisotropic thermal parameters were used for all non-hydrogen atoms except those of the solvent molecule. As it was not possible to locate clearly the positions of all the hydrogen atoms, they were placed at their geometrically calculated positions and included in the final structure calculations with fixed isotropic thermal parameters ($B = 7.0$ Å$^2$). The function minimized during the refinements was $\sum w|\Delta F|^2$. Unit weights were used in all stages of the refinement for **2**, whereas a weighting scheme $w = K[\sigma^2(F_o) + gF_o^2]^{-1}$ was used in the last cycles of refinement for **3**, at convergence the values for $K$ and $g$ being 0.4205 and 0.0033, respectively. The final $R$ and $R_w$ values were 0.080 and 0.098 for **2** and 0.045 and 0.055 for **3**, respectively ($R = \sum(|F_o| - |F_c|)/\sum(|F_o|)$ and $R_w = [\sum w(|F_o| - |F_c|)^2/\sum w(|F_o|)^2]^{1/2}$. The scattering factors were taken from ref 76, except those of the hydrogen atoms, which were taken from ref 77. Corrections for the real and imaginary components of the anomalous dispersion were made for Pt and P atoms.[77] Final atomic coordinates for the significant atoms of **2** and **3** are listed in Tables 6 and 7. All calculations were carried out on the CRAY X-MP/12 computer of the Centro di Calcolo Elettronico Interuniversitario dell'Italia Nord-Orientale (CINECA, Casalecchio Bologna, Italy) and on the GOULD-SEL 32/77 computer of the Centro di Studio per la Strutturistica Diffrattomerica del CNR, Parma, Italy.

**Table 6.** Fractional Atomic Coordinates ($\times 10^4$) with Esd's in Parentheses for the Significant Atoms of **2**

| atom | $x/a$ | $y/b$ | $z/c$ |
|---|---|---|---|
| Pt(1) | 0 | 1689(2) | 2500 |
| Pt(2) | −808(1) | 504(1) | 2567(7) |
| P(1) | 1022(8) | 1741(12) | 2593(25) |
| P(2) | 0 | −297(11) | 2657(41) |
| P(3) | −1622(7) | −186(10) | 2278(9) |
| C(1) | 0 | 2817 | 2585 |

**Table 7.** Fractional Atomic Coordinates ($\times 10^4$) with Esd's in Parentheses for the Significant Atoms of **3**

| atom | $x/a$ | $y/b$ | $z/c$ |
|---|---|---|---|
| Pt(1) | 0 | 1371(1) | 2500 |
| Pt(2) | 435(1) | 2738(1) | 1973(1) |
| P(1) | 1114(1) | 3321(2) | 1447(2) |
| P(2) | 0 | 3629(2) | 2500 |
| P(3) | 355(1) | 1585(1) | 1506(2) |
| C(1) | 1031(6) | 3087(6) | 490(6) |

**Raman Spectroscopy.** The Raman spectra were recorded on two different spectrometers. The first one was a Bruker IFS66/CS FT-IR spectrometer coupled with an FRA106 FT-Raman module using a Nd:YAG laser (1064 mm excitation) and a Notch filter (cutoff ∼60 cm$^{-1}$). The spectra were acquired using 200−300 scans and a 4 cm$^{-1}$ resolution. The laser power applied at the sample was typically 100 mW. The second instrument was an ISA Raman spectrometer equipped with a U-1000 Jobin-Yvon 1.0 m double monochromator using the 488.9−514.5 nm blue and green lines of a Spectra-Physics argon ion laser or using the 637.0 nm red line of a Spectra-Physics krypton ion laser. For each sample, one or two scans were acquired using the 32× microscope objective, 1 s/point, 1 point/cm$^{-1}$, no smoothing, and typically 10−30 mW laser power at the sample.

**Computational Details.** The parameters used in the extended Hückel calculations for the platinum atoms were taken from ref 78. The modified Wolfsberg−Helmholz formula[79] was used throughout this work. The geometries used for the cluster calculations were somewhat idealized from the experimental ones, using for instance $D_{3h}$ and $C_{2v}$ geometries for the two isomers. Bond lengths used were Pt−Pt = 2.755 Å, Pt−P(terminal) = 2.24 Å, Pt−P(bridging) = 2.25 Å, Pt−C = 1.97 Å in the closed geometry and 2.05 Å in the open one (as experimentally found), P−H($PH_3$) = 1.42 Å, P−H($PH_2$) = 1.438 Å, and C−H = 1.09 Å.

**Acknowledgment.** P.B. and R.B. gratefully acknowledge support from the Centre National de la Recherche Scientifique and, together with E. S. and A. T., the Commission of the European Communities (Contract No. CHRX-CT93-0277), and P.D.E. and B.H. thank the National Science Foundation for partial support of this work via Grant CHE8921632. We thank Johnson Matthey PLC for a generous loan of $PtCl_2$. We are grateful to Dr. J.-F. Halet (University of Rennes, France) for providing us with the contour maps.

**Note Added in August 1995.** Since this paper was first submitted (Oct 1990), relevant publications have appeared in the literature that should have been cited in Table 3.[80]

**Supporting Information Available:** For **2** and **3**, listings of all refined atomic coordinates (Tables S-1 and S-2), hydrogen coordinates (for **3** only; Table S-3), thermal parameters (Tables S-4 and S-5), and experimental data for the X-ray diffraction study (Table S-6) (6 pages). Ordering information is given on any current masthead page.

IC951164X

(76) Walker, N.; Stuart, D. *Acta Crystallogr., Sect. A: Cryst. Phys., Diffr., Theor. Gen. Crystallogr.* **1983**, *A39*, 158−166. Ugozzoli, F. *Comput. Chem.* **1987**, *11*, 109−120.

(77) *International Tables for X-Ray Crystallography*; Kynoch Press: Birmingham, England, 1974; Vol. IV.

(78) Summerville, R. H.; Hoffmann, R. *J. Am. Chem. Soc.* **1976**, *98*, 7240.

(79) Ammeter, J. H.; Bürgi, H. B.; Thibeault, J. C.; Hoffmann, R. *J. Am. Chem. Soc.* **1978**, *100*, 3686.

(80) (a) Puddephatt, R. J.; Manojlovic-Muir, L.; Muir, K. W. *Polyhedron* **1990**, *9*, 2767. (b) Burrows, A. D.; Mingos, D. M. P. *Transition Met. Chem.* **1993**, *18*, 129.